

# Master Thesis

High pressure dynamic seal development for SOCCS flow-return tube

M. van Arkel



# Master Thesis

High pressure dynamic seal development for  
SOCCS flow-return tube

by

M. van Arkel

to obtain the degree of Master of Science  
at the Delft University of Technology,  
to be defended publicly on April 20, 2016.

Student number:	1516175	
Project duration:	June 29, 2015 – April 20, 2016	
Thesis committee:	Prof. dr. A. V. Metrikine,	TU Delft
	Dr. Ir. R. A. J. van Ostayen,	TU Delft
	Ir. A. Jarquin Laguna,	TU Delft
	Ir. P. C. Kriesels,	Shell
	Ir. S. Sotskiy,	Shell

*This thesis is confidential and cannot be made public until April 20, 2021.*

An electronic version of this thesis is available at <http://repository.tudelft.nl/>.



# Abstract

Over the last couple of years, the Wells R&D department has developed a new concept for well construction: Shell Open Hole Continuous Casing System (SOCCS). The main characteristic of the concept is that the well design will not consist of a tapered structure, but rather a single diameter in casing used over its entire length. This new technology brings new challenges: one of these is to design a high pressure dynamic seal.

The purpose of is to seal of the space between the moving casing and the flow-return pipe against a kick, which can occur during drilling. It is also necessary to pressure test the longitudinal weld on the SOCCS casing during movement, therefor a fluid is pumped between a set of seals up to 200 bar. The designed seal should be capable of holding the pressure at minimum leakage, whilst also having a low friction force on the SOCCS casing.

This study was conducted to provide insight into different techniques to design a high pressure dynamic seal. Due to the wide range in different technique, this research touches upon many different sciences, ranging from Material Science, Chemistry, Fluid mechanics, System & Control, Tribology etc. The study presents an overview of the different techniques that are used in the industry for similar problems together with new ideas for sealing concepts. After an analysis of the most promising concepts a selection is made which will be subjected to experimental testing. During the research an experiment set-up is designed to subject these concepts to similar conditions as in real life. Finally the data of these tests are analyzed and the solutions are discussed.

A total of four concepts were selected to undergo full-scale experimental testing: Non-Newtonian Yield Stress Plug, Swellable Rubber, Chevron seal and Compression packing. For the first concept a mixture containing water, salts and laponite is chosen, after reacting through a precipitation reaction a very viscous fluid forms. Tests have shown that the shear-thinning effect of the fluid is so dominant that the fluid actually moves as a plug through the gap. The achieved pressure was considerably lower than expected and at high pressure the system becomes unstable. Certain explanations are provided to explain this behavior; furthermore CFD simulations are performed and have shown as a good tool to model the flow. How the CFD simulation does not incorporate the unstable behavior at high pressure, therefore it is advised to first investigate the instability further.

The test with the swellable rubber actually had to be cancelled before it was ready. Due to the bleeding of the SAP out of the rubber, the swell rate of the rubber decreased in comparison with small scale tests. Some beginning research for an oil swellable rubber was also performed; initial small scale test indicated much faster swell rates in comparison with water. Experiments to enhance the rheology properties of the oil have also been conducted and show promising results. Not only is it possible to increase to viscosity to a desired value, but the fluid displays a Newtonian behavior.

The test with Chevron seals was inadequate to say anything about their behavior as a high pressure dynamic seal. Due to a fault in design a not properly working seal was tested. It is recommended to still perform these tests.

Experiments with water in combination with compression packing showed that the concept was able to hold pressure during static conditions up to 48 bar at a flowrate of 50 ml/min, but during movement of the SOCCS casing the packing material got extruded out of the housing, holding almost no pressure. For the testing with wireline fluid, almost Newtonian like fluid with viscosity of 1000 cP, anti-extrusion rings were also added. It was clear that both adaptations increased the performance of the seal; eventually it was able to hold a pressure of 200 bar at a flowrate of approximately 10 ml/min, with a friction force of around 4 kN. This falls well within the set requirements for the design of the seal and out of all concepts is the closest to implementation in the field.

It is recommended to continue on the work concerning oil-based fluid; this would benefit the performance of all concepts. Because is it easier to control the rheology properties of this fluid then with a water-based fluid and it acts more or less as an Newtonian fluid. Furthermore the next steps should be taken in the final design of the seal; the compression packing would be the quickest way to develop a final design.



# Preface

This thesis report is the product of ten months working at the Shell offices in Rijswijk or Amsterdam and Delft University of Technology.

This graduation project was a combination of practical, experimental and theoretical work. Through I have been able to learn a lot about sealing mechanisms, chemistry, rheology, tribology, fluid dynamics, experimental design and stakeholders management. Almost all of these aspects were very new for me and enabled me to have a very steep learning curve. To be able to learn so much in a short time was only possible with the help from my colleagues in Wells R&D who are extremely helpful, patient and knowledgeable. I am very grateful to have been part of the team, if only for a short amount of time.

Naturally, I would like to thank Pierre Kriesels and Sergey Sotskiy for the opportunity to perform my graduation at the Wells R&D department of Shell in Rijswijk. Together they guided me throughout the entire project and supported me during the weekly meetings. Their knowledge and patience helped me to understand the sometimes unfamiliar physical problems along the way. From the start I felt appreciated as a part of the team and they gave me a high responsibility and were very open towards my own input about the project. This openness was extremely motivating and I really enjoyed working together, therefore I look back at a successful but above all fun ten months.

Since the project also involved a lot of practical work concerning the construction of the experimental set-up, I would like to thank all the people involved from both the Wells R&D department and the support staff from Experimental Services. I believe I asked almost everyone from those departments for help, ranging from a simple question to working extensively on the project together. In particular I would like to point out Cor Taal, Rob Neiteler and Alex Schwing, who helped me with the design and construction of the set-up. During the first few months of the project they put in a great deal of work trying to realize my sometimes incomplete ideas, without them I would never be able to achieve a fully working experimental set-up.

A special thanks goes out to Erik Cornelissen and Wouter Besijn, who have been a continuous help during the entire project. Erik taught me the basic principles of rheology and acted as a very valuable coach throughout the project. Wouter was irreplaceable during the project, with his extensive knowledge of the project and experimental experience he showed me the ropes of experimental work. Both of them gave me the responsibility to make my own decisions and taught me to see the implications of those decisions. A large amount of patience was also important; since they let me experiment with an idea even if they already knew it would not be successful. This way of working allowed me to get the most out of my time at Shell.

I would also like to thank the people from the university in the graduation committee. Antonio Jarquin Laguna for the more extensive help during the meetings at the university and lessons learned concerning experimental work. Ron van Ostayen played an important role in understanding the mechanisms of every separate sealing concept and is help with the CFD simulation. Last I would like to thank Andrei Metrikine for agreeing to be my supervising professor, even if the graduation topic touched upon a lot of topics outside structural dynamics he was still able to provide me with a better insight in the experimental results.

Last but not least, I would like to thank my friends and family for their support, especially my co-interns Govert, Daan, Albert, Floris, Ilsa, Pjotr, Wouter and Marc, who were a constant source of motivation during the past ten months.



*M. van Arkel*  
Delft, 8<sup>th</sup> April 2016



# Nomenclature

## List of Acronyms

AH	Alongside Hole
BC	Boundary Conditions
BOP	Blowout preventer
CF	Controlled Flowrate
CFD	Computational Fluid Dynamics
CP	Controlled Pressure
CR	Controlled Shear Rate
CS	Controlled Shear Stress
ELECTRE	Elimination and Choice Expressing Reality
IC	Initial Conditions
ID	Inner Diameter
MCDA	Multiple Criteria Decision Analysis
NDM	Novel Drilling & Materials
NDT	Non Destructive Testing
OD	Outer Diameter
PID	Proportional Intergral Derivative
PL	Power-Law Model
PTFE	Polytetrafluoroethylene
R&D	Research & Development
SAP	Super-absorbent Polymer
SOCCS	Shell Open Hole Continuos Casing System
TVD	True Vertical Depth

## List of Symbols

$A$	$[mm^2]$	Area
$\delta$	$[J^{1/2}m^{-3/2}]$	Solubility parameter
$D$	$[mm]$	Diameter
$E$	$[N/mm^2]$	Elasticity Modulus
$\eta$	$[Pa * s]$	Viscosity
$F_b$	$[N]$	Buckling Force
$H_v$	$[J]$	Heat of Evaporation
$i$	$[-]$	Dimensionless Correction Factor
$I$	$[mm^4]$	Moment of Inertia
$L_{eff}$	$[m]$	Buckling Effective Length
$M$	$[mol/ltr]$	Molar Mass
$[M]$	$[mol/ltr]$	Molarity
$\mu$	$[Ns/m^2]$	Dynamic Viscosity
$p$	$[bar]$	Pressure
$P$	$[Pas]$	Dynamic Viscosity in Poise
$\Pi$	$[bar]$	Osmotic Pressure
$Q$	$[m^3/s]$	Flow
$r$	$[mm]$	Radius
$R$	$[\Omega]$	Electrical Resistance
$R_{gas}$	$[Jmol^{-1}K^{-1}]$	Gas Constant
$R_g$	$[mm]$	Radius of Gyration
$S$	$[-]$	Slenderness Ratio

---

$S_{cr}$	[-]	Critical Slenderness Ratio
$s$	[ $m$ ]	Distance
$\sigma_y$	[ $N/mm^2$ ]	Yield Strength
$t$	[ $s$ ]	Time
$T$	[ $K$ ]	Temperature
$T_g$	[ $K$ ]	Glass-transition Temperature
$\tau$	[ $Pa$ ]	Shear stress
$v$	[ $m/s$ ]	Velocity
$V$	[ $V$ ]	Electric Potential
$V_m$	[ $dm^3/mol^{-1}$ ]	Molar Volume
$\gamma$	[ $1/s$ ]	Shear rate

# Contents

<b>1</b>	<b>Introduction</b>	<b>1</b>
1.1	Business Case . . . . .	1
1.2	Introduction to drilling technologies . . . . .	1
1.2.1	Conventional drilling . . . . .	1
1.2.2	Well Control . . . . .	2
1.3	SOCCS . . . . .	3
<b>2</b>	<b>Project Overview</b>	<b>5</b>
2.1	Problem statement . . . . .	5
2.2	Thesis objectives . . . . .	6
2.3	Structure of Thesis . . . . .	7
<b>3</b>	<b>Approach</b>	<b>9</b>
3.1	Design of Seal . . . . .	9
3.1.1	Functional requirements. . . . .	9
3.1.2	Geometry . . . . .	9
3.1.3	SOCCS casing . . . . .	10
3.1.4	Weld . . . . .	10
3.1.5	Surface roughness . . . . .	11
3.1.6	Sealing Concepts. . . . .	11
3.2	Concept Derivation Methodology. . . . .	13
3.2.1	Requirements . . . . .	13
3.2.2	Criteria. . . . .	13
3.2.3	ELECTRE Method . . . . .	14
<b>4</b>	<b>Detailed Concept Design</b>	<b>15</b>
4.1	Non-Newtonian Yield Stress Plug . . . . .	15
4.1.1	Precipitation Reaction . . . . .	15
4.1.2	Final Design . . . . .	16
4.2	Swellable Rubber . . . . .	17
4.2.1	Swell Rates. . . . .	17
4.2.2	Final Design . . . . .	18
4.3	Compression Packing. . . . .	18
4.3.1	Final Design . . . . .	18
4.4	Chevron/V-Packing . . . . .	19
4.4.1	Final Design . . . . .	19
<b>5</b>	<b>Results &amp; Discussion</b>	<b>21</b>
5.1	Non-Newtonian Yield Stress Plug . . . . .	21
5.1.1	Test Results . . . . .	21
5.1.2	Instability . . . . .	22
5.1.3	Model comparison with experiments . . . . .	24
5.1.4	Data Fitting . . . . .	25
5.1.5	Discussion . . . . .	26
5.2	Swellable Rubber . . . . .	26
5.2.1	Test Results . . . . .	26
5.2.2	Discussion . . . . .	28
5.2.3	Oil Swellable Rubber. . . . .	29
5.3	Compression Packing. . . . .	30
5.3.1	Test Results . . . . .	30
5.3.2	Discussion . . . . .	34

5.4	Chevron Seal . . . . .	35
5.4.1	Test Results . . . . .	35
5.4.2	Discussion . . . . .	36
<b>6</b>	<b>Conclusions</b>	<b>39</b>
<b>7</b>	<b>Recommendations</b>	<b>41</b>
7.1	Recommendations for Future Research . . . . .	41
7.2	The Way Forward for Shell . . . . .	42
	<b>Bibliography</b>	<b>43</b>
<b>A</b>	<b>Concepts Overview</b>	<b>45</b>
A.1	Contact Seals . . . . .	45
A.1.1	Elastomer Seals . . . . .	45
A.1.2	Packing Seals. . . . .	46
A.1.3	Swellable Rubber. . . . .	47
A.2	Clearance Seals . . . . .	48
A.2.1	Labyrinth Seal . . . . .	49
A.2.2	Brush Seal . . . . .	49
A.2.3	Non-newtonian Yield Stress Plug. . . . .	50
A.2.4	Ferro-Fluid Seal . . . . .	53
<b>B</b>	<b>Concept Derivation Methodology</b>	<b>55</b>
B.1	Criteria Evaluation . . . . .	55
B.2	Concept Evaluation . . . . .	56
<b>C</b>	<b>Experiment Set-Up</b>	<b>57</b>
C.1	Structural design . . . . .	57
C.1.1	Pressure chamber . . . . .	57
C.1.2	Dynamic actuator . . . . .	57
C.1.3	Stinger design . . . . .	58
C.2	Measurement environment . . . . .	59
C.2.1	Friction . . . . .	60
C.2.2	Leakage . . . . .	60
C.2.3	Additional measurements . . . . .	63
C.3	Experimental Set-Up Calculations . . . . .	64
C.3.1	Buckling force in stinger . . . . .	64
C.3.2	Thermal energy due to friction. . . . .	65
C.3.3	Deformation of SOCCS casing . . . . .	65
<b>D</b>	<b>Non-Newtonian Yield Stress Plug CFD</b>	<b>67</b>
D.1	CFD Simulations . . . . .	67
D.1.1	Assumptions. . . . .	67
D.1.2	Results . . . . .	68
D.1.3	Dynamic conditions . . . . .	69
D.2	Model. . . . .	70



# Introduction

In the introduction additional information is given on the business case of SOCCS, how conventional wells are drilled and an introduction to SOCCS. Thereafter the main objective of this thesis is presented.

## 1.1. Business Case

The ability to drill using a continuous casing system has great potential in developing a more cost effective way of well construction. The goal of this technology is to decrease well construction costs, by eliminating casing running time; reducing amount of materials used for well construction; less cuttings produced and less drilling mud is required. The SOCCS system enables the driller to simultaneously produce the casing while drilling resulting; in a higher well construction speed.

Future development of this technology may allow a revolution in how the industry constructs wells. This can eventually translate into drilling in a more cost effective way while having the same quality safety standards as conventional drilling technologies.

At this moment a prototype of this system is deployed in Joure, in the northern part of the Netherlands. The machine is able to form and invert the pipe, with a ID of 4" and a wall thickness of 3.4 mm. During a drill test in October/November of 2015, new records were achieved:

- Bit depth = 433 m TVD, 643 m Alongside Hole (AH)
- Casing depth = 391 m TVD, 597 m AH

It still remains to be seen if Shell will continue to develop this technology on its own. Due to shift in focus of the Wells R&D department other technologies are higher in priority. Shell still has the commitment to find a commercial partner in order to further develop this new drilling technology. If proven useful this research will contribute to the designing of the overall SOCCS technology.

## 1.2. Introduction to drilling technologies

### 1.2.1. Conventional drilling

A typical oil or gas well can be several kilometers deep [2]. When drilling so deep, one encounters various layers of rock. Each formation layer has different properties, *e.g.* strength, composition, pore pressure and permeability. To cope with these formation changes, a well is drilled in several sections. A string of casing is run in the drilled borehole to seal off the formation and to prevent collapse of the borehole. This casing string is cemented in place for integrity and to provide a barrier between the reservoir and different earth layers. From that point on a smaller bit is used and the well is drilled further. When again an unstable depth is reached, the borehole is cased and the drilling-cycle repeats. This will be done multiple times before the desired depth is reached, leaving the well with a telescopic character. This effectively means that in order to reach the necessary depth the diameter in the beginning is wider than at the end. In the case of a single diameter along the entire well, it would greatly reduce produced cuttings and required drill mud. A side-view of the intersection along the axial length of a conventional telescopic well design is presented in figure 1.1.

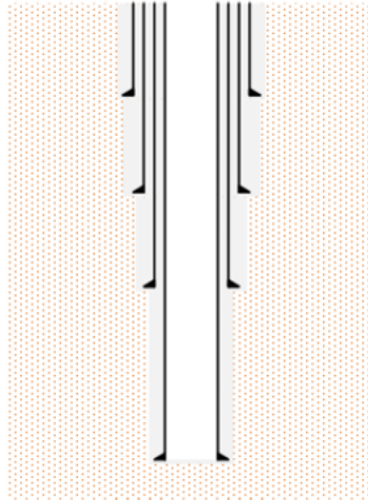


Figure 1.1: Schematic lay-out of conventional drilled well

### 1.2.2. Well Control

During drilling operations it is important to control the well. Controlling the well involves regulating the pressure down hole by pumping drilling mud down, see figure 1.2 for an overview of mudflow through a well. This has multiple reasons:

1. The liquid cools the drill bit
2. The fluid flow transport the cuttings from down hole to the top of the well
3. The fluid column in the well acts as a hydrostatic column to keep pressure on the well

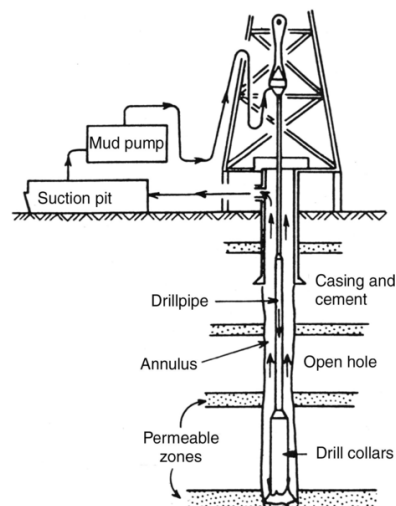


Figure 1.2: Circulation of mudflow in well

The drilling fluid is pumped under pressure into the well and therefore it moves towards an area with a lower pressure, which is at the top of the well. At the top of the well the Blowout Preventer (BOP) is located, an example is shown in figure 1.3. This device is capable of sealing the well around the casing or the drill pipe; it is even possible to completely shear the casing/drill string. A BOP is an essential tool of a well. Failure of a BOP can lead to catastrophic events (e.g. Deepwater Horizon [8]). Due to technology specific requirements with the SOCCS equipment, additional measures are taken to ensure certain leak paths are blocked.

The rams on the lower part of the BOP act as seals when activated. When the rams are closed it is possible to control pressure in the well using mud returns, kill and chokes to regulate flow. From figure 1.3 it becomes

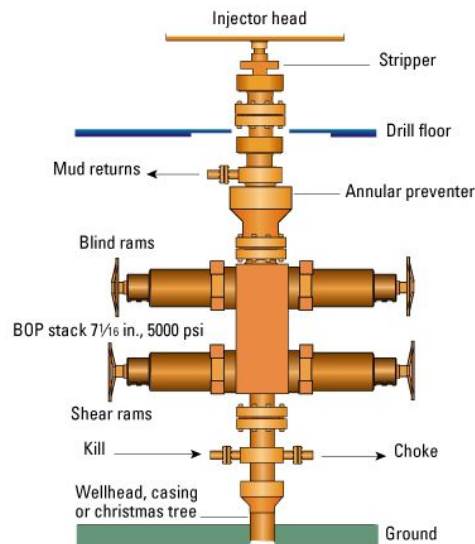


Figure 1.3: Schematic overview of BOP

clear that the BOP is placed directly on top of the wellhead, so the BOP also ensures a safe working environment for the people on top of the drill floor. The SOCCS technology makes use of a conventional BOP, but because it has to be positioned different from a conventional drilling operation additional dynamic seals need to be in place. This is described further in section 1.3.

### 1.3. SOCCS

SOCCS is a new well construction technology developed by Shell. The main idea behind this construction technique is to produce the casing while simultaneously drilling the well. This enables the driller to construct the well quicker than when using a conventional drilling system. Another important advantage of this technology is that there is no tapered well design, but a single casing diameter alongside the whole length of the well. In figure 1.4 a general idea of the increase in well construction time that can be obtained is displayed.

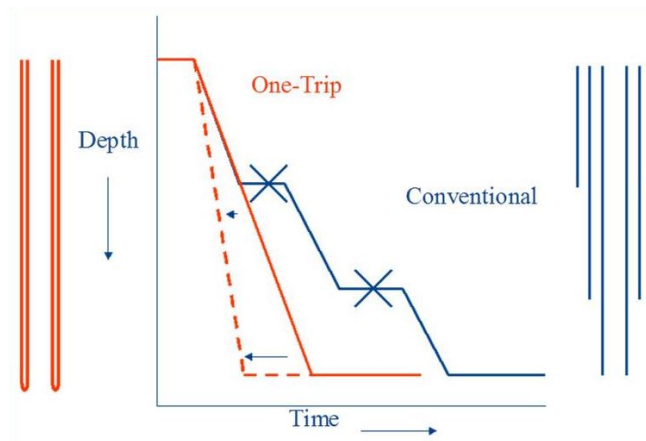


Figure 1.4: SOCCS vs. conventional drilling time

In order to produce the casing simultaneously while drilling, the casing is inverted while the borehole is drilled. This is done by putting a force on the inner pipe, which then inverts at its lowest point. The outer part of the casing is stationary during the drilling process and therefore there is no friction between the outer part of the casing and the borehole. An overview of this process is given in figure 1.5.

In figure 1.6 a total overview of the SOCCS drilling technology is given. In the top of the figure the casing is formed from a steel plate, which is supplied on a coil. The steel plate moves through the pipe mill which

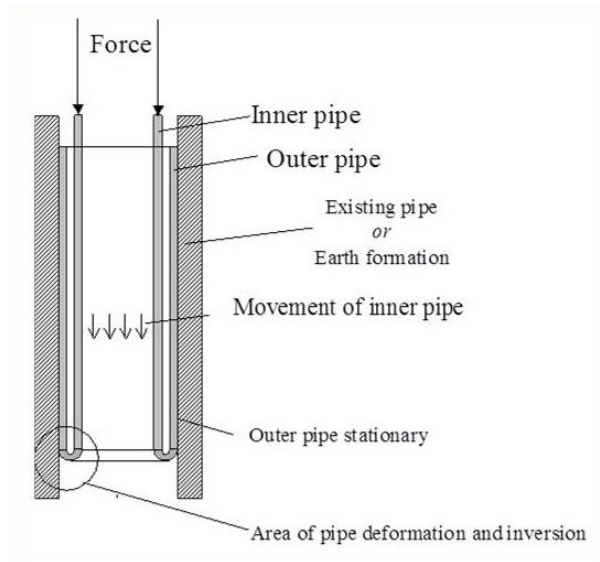


Figure 1.5: Inversion process of the casing

plastically deforms the plate into a steel pipe. The casing is then welded at the top, in longitudinal direction, using a laser welding machine. Afterwards the casing moves through the pipe tractor which supplies the necessary pulling/pushing force on the pipe to move it through the pipe mill and push it down the hole where it eventually inverts, while also overcoming the friction between the inner and outer pipe.

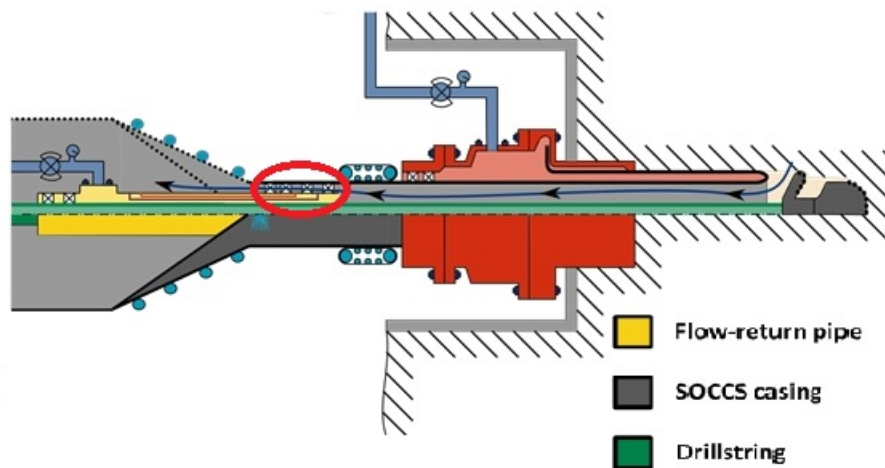


Figure 1.6: Schematic overview of SOCCS concept

There are 2 pipes running through the casing: a drill string and the flow-return pipe, as shown with the colors in figure 1.6. The drill string runs all the way to the bottom of the well and is powers the drill bit. The flow-return pipe runs 4-5 m after the welding point, after which it stops. The function of the flow-return pipe is to guide the drilling fluid with the cuttings; no cuttings or fluid should pass through the annular gap between the flow-return pipe and the moving casing. It is the goal of this research to find a solution to block this leak path between the 2 pipes. The location of the seal is highlighted by the red circle in figure 1.6.

# 2

## Project Overview

In this section a more elaborate description will be given concerning the actual problem of the thesis, followed by an overview of the thesis objectives. Finally the structure of the report will be mentioned.

### 2.1. Problem statement

As mentioned in section 1.2.2 and section 1.3, additional dynamic seals need to be present in the SOCCS technology. The question is raised: How to block the leakage path (see figure 1.6) between the flow-return pipe and moving SOCCS casing be blocked during drilling? A seal has to be designed to fit in the annular gap between the flow-return pipe and the casing, figure 2.1.

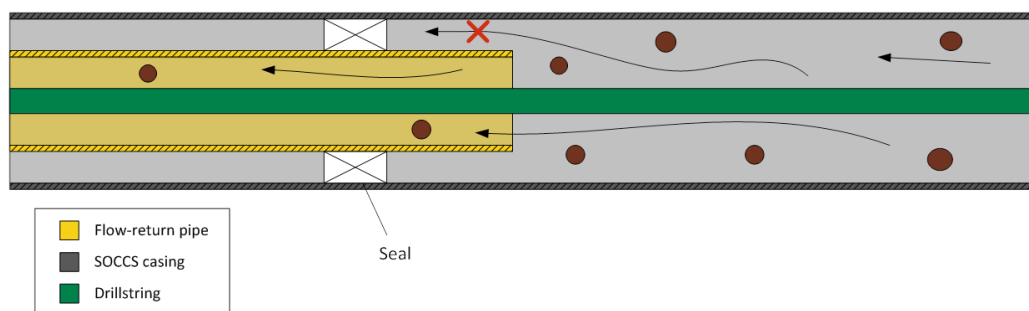


Figure 2.1: Blocking of leakage patch due to seal

The casing is welded in the longitudinal direction, this is done on the surface. The weld is tested with a Non-Destructive Testing (NDT) system, due to regulations it is also necessary to pressure test the weld. Any fault in the weld should be detected above ground, when the casing is pushed in the ground it is not possible to make any repairs on the weld. In order to pressure test the weld a system of 2 seals is used, with a pressurized fluid in between, see figure 2.2.

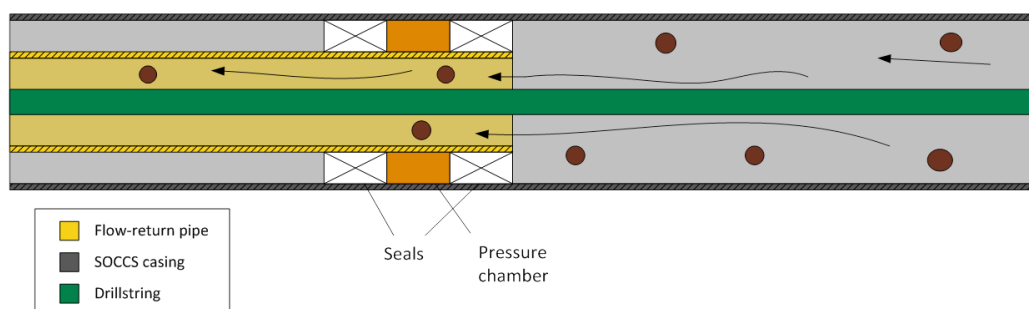


Figure 2.2: Intersection of conventional drilled well

This seal system needs to be designed to withstand operational conditions, such as:

- Speed of casing
- Geometry & roughness of casing
- Acceptable friction
- Acceptable wear
- Acceptable leakage
- Pressure

The problem statement is to develop a seal system which can perform under these environmental and operational conditions during drilling. The functionality of the seal is to block the leakage path between the flow-return pipe and the SOCCS casing while pressure testing the weld. Because the geometry of the SOCCS pipe and the flow-return pipe present a difficult challenge to design a seal without leakage, a certain amount of leakage is accepted.

## 2.2. Thesis objectives

As mentioned in the previous paragraph the objective of the thesis is to develop a better understanding of dynamic sealing concepts, for well control and pressure testing of the weld. In order to design it is important to learn about the current methods used in the industry; this will be part of the literature study in the research. Besides readily available concepts new techniques to seal off the gap are also discussed.

Afterwards multiple concepts should be evaluated and with help of a methodology the promising concepts should be further designed. Apart from the theory it is also required to design a test set-up, in which it is able to test a range of different concepts. During the experiments data will be obtained through measurements in order to analyze the behaviour of the concepts.

From these experiments conclusions and recommendations can be made on the performance of each concept. It is not the goal of the study to compare the results between different concepts, since each concept works according a different principle. In the end only a final advice will be given to Shell what is possible to improve on every concept, recommendations for further research on how to understand certain concepts is also provided. Below the objectives are summarized together with the corresponding questions that need to be answered:

- Understand current sealing principles and create an overview of different sealing techniques
  - Which physical principles are relevant to seals?
  - What different techniques are used in the industry or other industries for a similar problem?
  - Are there any new techniques available?
- Develop a concept derivation methodology
  - How are the sealing concepts ranked?
  - Which assumptions need to be made to work these out?
  - Which promising concepts are good enough to go through experimental testing?
- Design an experimental set-up
  - How should the test set-up relate to the operations in real-life?
  - What environmental parameters should be included?
  - What measurements should be obtained during the experiments and how should they be obtained?
- Test various sealing concepts with experiments
  - What are the most important parameters influencing the measurement? How do they influence the design?
  - What are the failure modes of each concept?
  - To what extent is the concept able to seal within the given requirements?

- Elaborate on results and evaluate
  - What is, in the end, the most promising concept and why?
  - What are the strengths, weaknesses, opportunities and threats of the design?
  - How can the design be implemented in a field trial? Or is there need for further research?

The outcome provides Shell with a firm understanding of different sealing techniques and a basis to develop a prototype which can be used in a field trial. The topics discussed in this thesis cover a wide range of different engineering aspects, e.g. Chemistry, Material Science and Fluid Mechanics. These topics are not directly related to courses in Offshore Engineering. Still the application of the technology is related to a well construction technique, which has some overlap with courses of the curriculum.

## 2.3. Structure of Thesis

The thesis is divided into seven chapters: (1) *Introduction*, (2) *Project Overview*, (3) *Approach*, (4) *Detailed Concept Design*, (5) *Results*, (6) *Conclusions* and (7) *Recommendations*. In the introduction (1) the basic concepts of drilling and SOCCS are already discussed. This chapter (2) the general problem statement of the thesis is described. From this problem statement a range of objectives and deliverables are derived. The corresponding questions will be answered in the remaining chapters of this thesis.

The approach chapter (3) provides a more thorough introduction to requirements for designing a seal. It also introduces the different concepts that are subjected to the concept derivation methodology.

After the decision which concepts are subjected to full scale testing the concepts need to be designed in more detail. This is done in chapter (4).

The results of the tests for the 4 concepts will be explained in the next chapter (5). In this chapter emphasize is given on the concept that has the most promising results. Most important is the validation of the data, to see if it corresponds with the expectations and the theory.

After evaluating the experiments conclusions are made concerning the validation of the experiments. Apart from the experiments conclusions on which concept would be most feasible are also given (6). Recommendations for further research and necessary steps before implementation in field trial are discussed in the final chapter (7).



# 3

## Approach

In section 3.1 the functional requirements for the design of the seal will be given, alongside with a more detailed view of the placement of the seal in the current SOCCS technology. This placement brings along certain difficulties for the design of the seal and they have to be taken into account in section 3.2, in which the concept selection will be discussed. It is also necessary to design and construct a test-up, Appendix C will describe this in more detail.

### 3.1. Design of Seal

The design of the sealing concepts depends on the functional requirements and geometry of the application in the SOCCS technology; both are discussed in the next two sections.

#### 3.1.1. Functional requirements

As discussed in chapter 2 the goal aim of the experiment is to test different sealing concepts in order to understand more of the dynamic behaviour of each concept. The most important operational conditions is that the fluid within the pressure chamber should be pressurized up to 200 bar. Because this drilling technology is designed to drill wells up to 2000 meters deep, the maximum kick that can be expected is 200 bar.

Apart from the pressure the other operational conditions are shown in table 3.1.

Table 3.1: Operational conditions

Operational conditions	Value
Speed of casing	1 [m/min]
Acceptable leakage	6 ltr/hour
Acceptable friction	+/- 10 kN
Acceptable wear	-
Geometry & surface roughness	-

In the table acceptable wear is left out intentionally, it is not regarded as measurable parameter in this thesis. Drilling is a single well will take around 4-5 km of casing, during which changing of a seal is not preferable. So a seal should be able to function properly along the entire length of the casing. In other words: leakage and friction should not change significantly over time. Geometry and surface roughness will be discussed in section 3.2.

#### 3.1.2. Geometry

From the start of the thesis it was clear the experimental set-up had to be able to test at a pressure of 200 bar. Because the Inside Diameter (ID) of the SOCCS casing is only 4", it was decided to do the experiments at real scale size. Therefore no scaling relations are needed for the experiments.

### 3.1.3. SOCCS casing

In the drilling process the SOCCS casing is formed in the pipe mill, due to the plastic deformation through rollers. Hence the formed casing does not have an perfect cylindrical shape, figure 3.1.

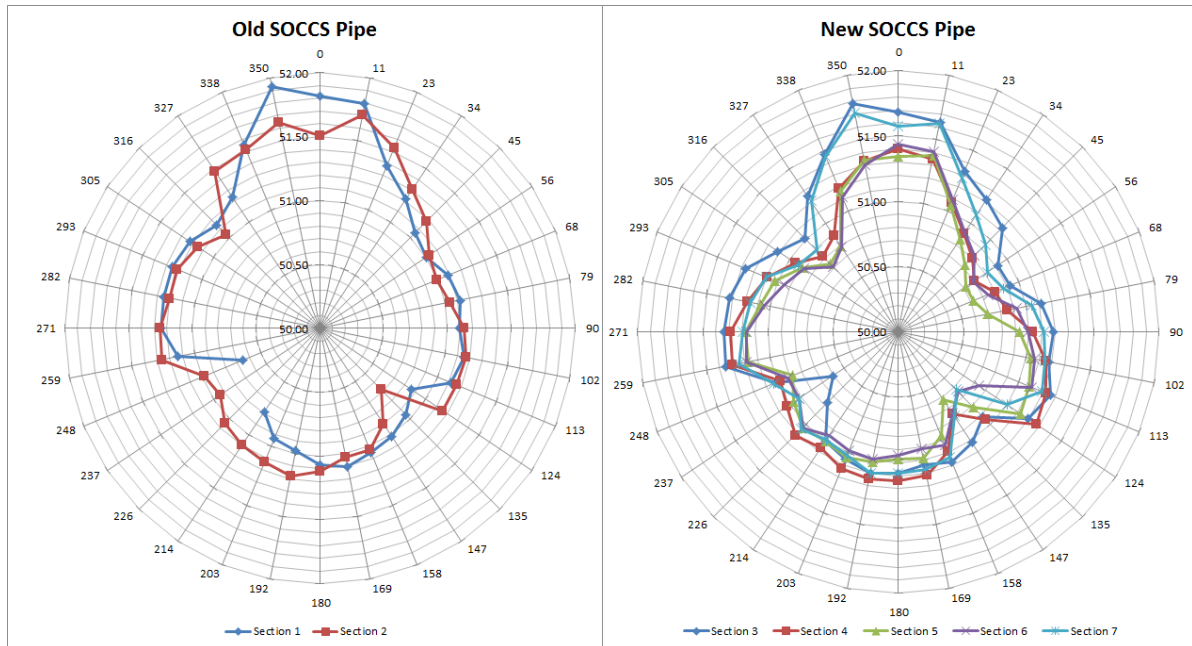


Figure 3.1: Out of roundness new & old SOCCS casing

On the circumferential axis in figure 3.1 the intersection of the SOCCS casing is plotted through degrees. The vertical axis represents the measured radius of the corresponding degree angle. The welded part of the casing is always displayed at angle  $0^\circ$  at the top of the graph, more on this in section 3.1.4. It can be concluded that the SOCCS casing has an out of roundness effect of around 1-2%. Figure 3.1 also shows different measurements taken in different sections; this corresponds to different sections of SOCCS casing along the axial length. The shape of the cross section in each section is rather constant and therefore small deviations in cross section in axial length of the SOCCS casing are neglected.

### 3.1.4. Weld

Another important geometry parameter is the weld in the casing. The weld is made by a laser and poses a serious problem for a seal. Under high pressures the weld can act as a saw cutting through material that comes into contact, therefore it needs to be investigated. In figure 3.2 a picture made by a light microscope is shown.



Figure 3.2: Light microscope image of weld

In figure 3.3 a 3D image is shown of the same weld. The data from this 3D image is used to measure the average height of the weld, which is approximately  $300 \mu\text{m}$ .

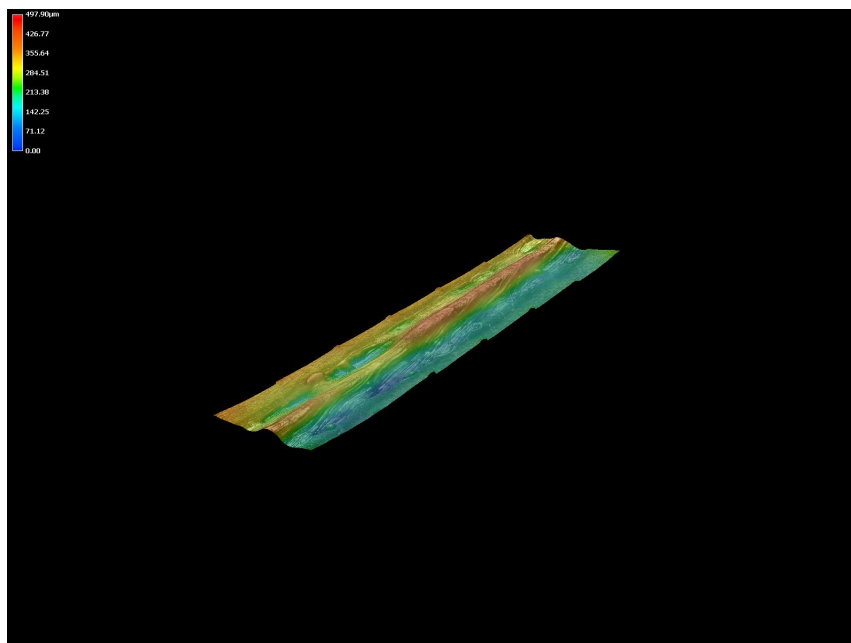


Figure 3.3: 3D image of weld

### 3.1.5. Surface roughness

The surface roughness is a component of surface texture and it is quantified by the deviations in the direction of the normal vector of a real surface from its ideal form. The most common used is the roughness average, or  $R_a$ , which is calculated by the formula:

$$R_a = \frac{1}{l} \int_0^l |f(x)| dx \quad (3.1)$$

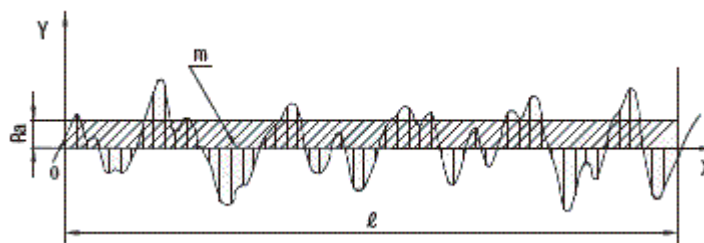


Figure 3.4: Average roughness of a surface

In figure 3.4 it is clear that the  $R_a$  value is a deviation from the mean surface of the material. The average roughness is directly related to friction and wear properties of the material. It is not assumed in the thesis that this property can be altered during the experiments. From earlier measurements the value of  $R_a$  is around 5 to 7, which is a relative high roughness for sealing applications.

### 3.1.6. Sealing Concepts

Sealing technologies covers a range of different techniques for all kinds of different applications. Generally sealing techniques are classified depending on field of application, as displayed in figure 3.5. In the case of SOCCS technology the focus is on dynamic seals, especially reciprocating shaft seals. Because the application in the SOCCS technology is not closely related to any existing applications, sealing technologies besides reciprocating shaft seals are also taken into account. Mainly due to the fact that in the SOCCS technology the seals will only be used in a one-direction motion, but the test set-up will have a reciprocating motion, as chosen in appendix C. Still reciprocating seals cover an extremely wide range of application, they are used in engines, cylinder, shock absorbers, hydraulic cylinders, pumps, compressors etc. [9].

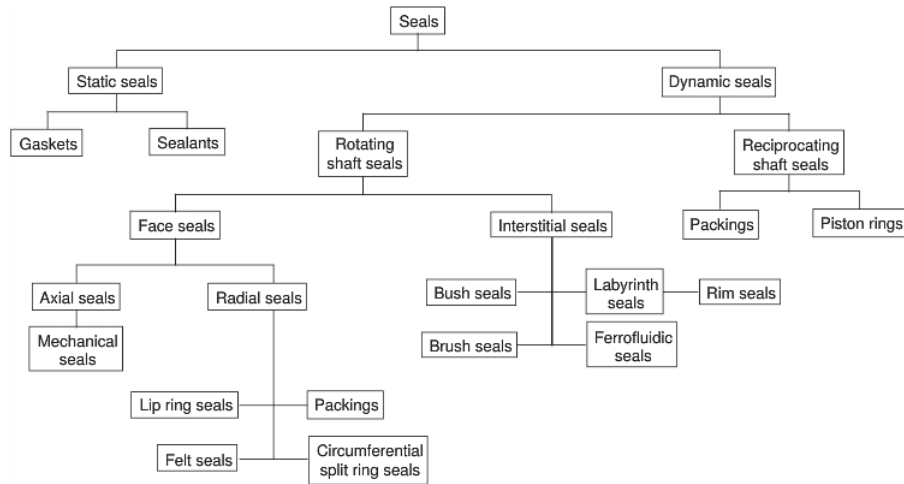


Figure 3.5: General seal classification chart

Dynamic seals have been optimized to provide both minimum leakage and minimum friction and wear, often mutually exclusive tribological objectives. Therefore is it common to divide the sealing techniques in the following categories:

1. Contact seals have the seal bear against its mating surface under positive pressure.
2. Clearance seals operate with positive clearance, meaning there is no sliding contact.

Whereas contact seals suffer mostly from high friction forces and clearance seals from high leakage. The majority of seals are contact seals, in which the seal is separated by a thin layer of lubricant (oil), see figure 3.6. How the seal is pressed against the rod depends on the thickness of the oil film and the fluid properties of the oil. Practically all seals, either static or dynamic, depend on the properties of the materials from which they are constructed and the interaction of the mating surfaces to achieve a reliable seal with minimum leakage. An overview of all concepts is given in Appendix A.

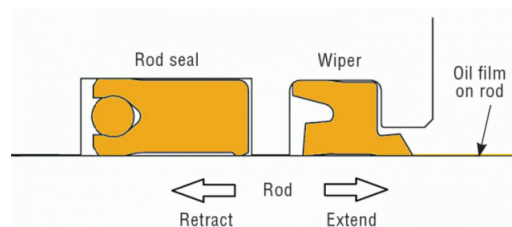


Figure 3.6: Example of a contact seal

In general the functionalities of any type of seal are:

- Contain pressure
- Retain or separate fluids
- Keep out contaminants

The functionalities above are also ranked in the order of importance with regard to the requirements of the to be developed seal. Sometimes a combination of different techniques is used to achieve the functionalities mentioned above. Figure 3.6 shows an example of a rod seal, where the rod seal itself is used to contain the pressure (located to the left of the rod seal in this picture). The wiper is used to retain or separate fluid and keep out contaminants. Additionally centralizing rings can be installed to ensure both shaft & rod or in the case of SOCCS the two pipes are properly aligned. In the remainder of this chapter only the main sealing technique is discussed, wipers and centralizers are not mentioned.

## 3.2. Concept Derivation Methodology

Now all the concepts have been introduced in section 3.1.2, it is time to determine which concepts have the most potential and that proceed through to the detailed engineering phase. In table 3.2 an overview is given of the concepts that will be taken into account.

Table 3.2: Overview of concepts

#	Contact Seals	#	Clearance Seals
1	O-ring	8	Labyrinth Seal
2	U-ring	9	Brush Seal
3	X-ring	10	Non-Newtonian Yield Stress Plug
4	Lip Seal	11	Ferro-Fluid Seal
5	Chevron / V-packing		
6	Compression Packing		
7	Swellable Rubber		

Since no concept has ever been tested, under these conditions nor are there any models available, a Multiple Criteria Decision Analysis (MCDA) has been used as a concept derivation methodology based on E. Pruyt [13], which is a tool that can support in concept selection. The goal of the analysis is the description, choice, ranking, classification or design of these alternatives on the different criteria [13]. The final outcomes of multiple criteria decision analysis are not end products, it is only a support tool. At the end the results need to be thoroughly reflected and questioned, from this evaluation a number of concepts should emerge that are ready to be designed for empirical testing.

### 3.2.1. Requirements

The requirements used in the MCDA corresponds with the design requirements mentioned in section 3.1 and repeated below in table 3.3. How every concept is capable of achieving these requirements is analyzed with help of the criteria in the next section.

Table 3.3: Operational conditions

Operational conditions	Value
Speed of casing	1 [m/min]
Acceptable leakage	6 ltr/hour
Acceptable friction	+/- 10 kN
Acceptable wear	-
Geometry & surface roughness	-

### 3.2.2. Criteria

According to Pruyt [13], the more criteria there are, the closer the concepts are equal to perform. Therefore the number of criteria should be kept to a minimum, whilst still evaluating the concepts on a broad spectrum of functionalities. The following criteria have been selected, see table 3.4.

Table 3.4: Operational conditions

Criteria
Wear
Coop with surface geometry
Coop with roughness
Leakage
Costs
Friction

The evaluation of the criteria is described in appendix B.

### 3.2.3. ELECTRE Method

The Elimination and Choice Expressing Reality (ELECTRE) method is used as a methodology to derive the most feasible concepts. The ELECTRE method is described in more detail in appendix B. The resulting scorecard is displayed in figure 3.7.

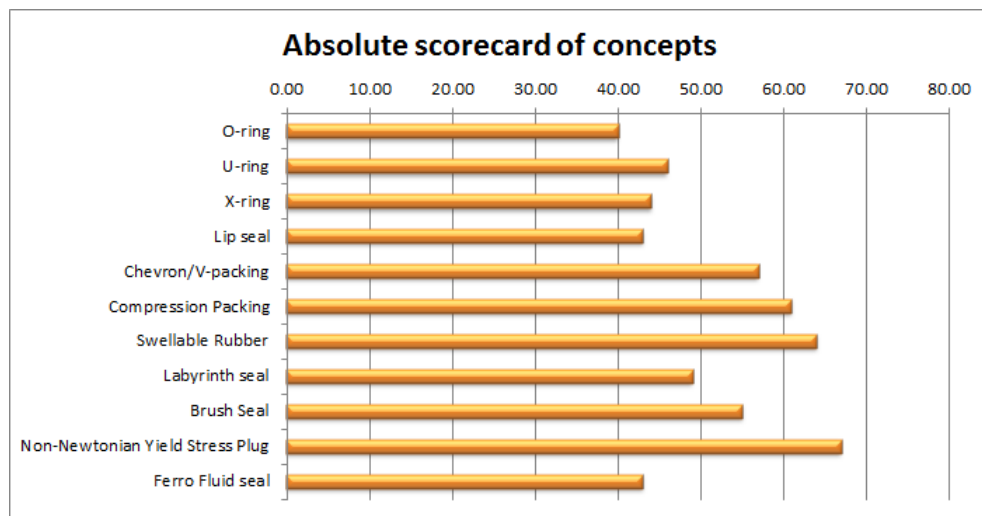


Figure 3.7: Absolute scorecard of concepts

The ELECTRE method is only a tool that helps with a decision, Pruyt [13], it is always necessary to discuss the results afterwards. The results are discussed for contact and clearance seals independently.

#### Contact Seals

From the contact seals concepts three concepts are clearly valued more feasible than the other concepts:

- Chevron/V-Packing
- Compression Packing
- Swellable Rubber

From literature it was quickly clear that the other concepts are not designed to withstand a pressure difference of 200 bar [5] [9]. The team had the confidence that the remaining three concepts also had better friction capabilities, because a larger range of different materials could be used. So the decision with help of Shell engineers was made to test all three of the most feasible concepts, since the differences between those concepts was minimal. The Compression Packing and Chevron/V-packing would be concept that can be ordered from a company, whilst the Swellable Rubber has to be made in-house.

#### Clearance Seals

From the clearance seals possibilities the Non-Newtonian Yield Stress Plug was obviously the most promising concept. Testing of this concept would also be useful since every concept will need a fluid and a more combinations of contact seals with this concept are possible. The Labyrinth seal was deemed as too similar to the Non-Newtonian Yield Stress Plug and hard to fabricate the tight clearances required. The team was convinced the Ferro Fluid seal was not possible to manufacture in the timescale. The Brush Seal was eliminated because it was also a time consuming concept, that in practice has never been in an application of 200 bar. A total of four concepts have been derived that will be further subjected to testing:

1. Non-Newtonian Yield Stress Plug
2. Swellable Rubber
3. Compression Packing
4. Chevron/V-Packing

# 4

## Detailed Concept Design

This chapter follows up from the theory stated in Appendix A, in which an introduction is provided on the different sealing concepts. In this chapter only the concepts chosen in section 3.2 are described in more detail. Because the concepts described in sections 4.1 and 4.2 are designed in-house, these will be explained in greater detail. The assumptions made in this chapter are put to the test in chapter 5.

### 4.1. Non-Newtonian Yield Stress Plug

As stated in Appendix A this concept is derived from the Hagen-Poiseuille principle used in wireline operations. Only now a Bingham Pseudoplastic (figure A.15) fluid is used, with a yield stress and shear thinning properties. Different viscosifiers have been taken into consideration to achieve a fluid with high viscosity. The decision was made to use Laponite as an additive to water, which consists of a layers of silicate discs, figure 4.1.

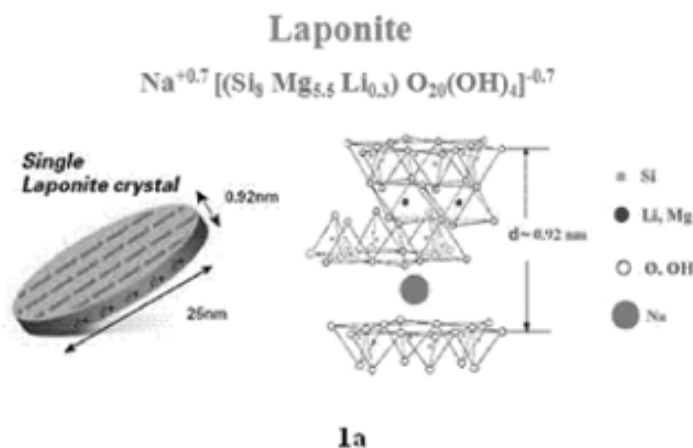


Figure 4.1: Molecule structure of Laponite

In order to reach the required viscosity it is necessary to at least use a mixture, with more than 10% laponite. Achieving a mixture with a higher percentage of laponite poses a problem, since the laponite directly increases the viscosity of the mixture. Therefore it is difficult to get a homogeneous distribution of all the laponite particles in the fluid, a solution for this discussed in section 4.1.1. The final design for the concept that is implemented in the full scale set-up is discussed in section 4.1.2.

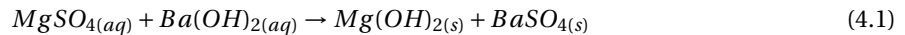
#### 4.1.1. Precipitation Reaction

A single laponite crystal has a disc shaped form when dissolved in water, with the top and bottom of the disc having a negative load and the side of the disc having a positive load. When dissolved in water these discs

form a interlinking structure, much like a house of cards. Because all the molecules line up in a structure a larger force is required to shear the fluid and thus creating a higher viscosity.

The solution to achieve mixtures with higher than 10% of laponite was found by using a precipitation reaction. When adding laponite to water, in which salt is dissolved, the viscosity does not increase drastically. To understand this it is important to look at the molecule structure in figure 4.1. The dissolved ions of a salt have a positive or negative electrical charge and they bind respectively to the contrary electrical loading on the laponite discs.

If the ions are electrically bound to the top/bottom and sides of the laponite crystal, it is not possible anymore for the laponite crystals to form a house of cards like structure. The ions prohibit laponite crystals from binding themselves to each other, thus the viscosity remains low. If a double precipitation reaction is used all of the ions react to form solids, named precipitate, this only leaves water with a high concentration of laponite. According to the solubility table in [17], a possible reaction could be as in equation 4.1.



The two salts need to be in the right ratio in order for all of the ions to react, if ions are left in the final mixture they would still partly prohibit the laponite to form its structure. The ratio is derived from the atomic weight of each salt, of  $Ba(OH)_2$  being  $171,43g/mol$  and  $MgSO_4$  has an atomic weight of  $120,37g/mol$ . The ratio in which the salt should be mixed is equal to the atomic weight divided by each other, equation 4.2.

$$ratio = \frac{atomic\ weight\ of\ Ba(OH)_2}{atomic\ weight\ of\ MgSO_4} = \frac{171.34}{120.37} \approx 1.42 \quad (4.2)$$

Next a closer look is taken to the solubility in water of both salts, with  $Ba(OH)_2$  having a solubility of  $3.89\ g/100\ ml$  and  $MgSO_4$  has a solubility of  $26.9\ g/100\ ml$ , both at a temperature of  $20^\circ C$ . Barium-hydroxide is the normative in this reaction, test in the lab showed a solubility rate of  $2\ gr/100\ ml$  is achievable. With the calculated ration in equation 4.2 this gives a desired concentration of  $MgSO_4$  of  $1.4\ gr/100\ ml$ .

#### 4.1.2. Final Design

Now the desired precipitation reaction is known, it is time to examine the desired fluid properties. To measure the the viscosity a Haake Mars 40 Rheometer is used, which can both operate shear stress controlled (CS) and shear rate controlled (CR) [3]. The measurements in figure 4.2 are done in the CS setting. The figure clearly shows that for very low shear rates the fluids has a very high shear stress and acts as a solid. After it passes over the yield stress the shear rate increases and the resulting viscosity drops.

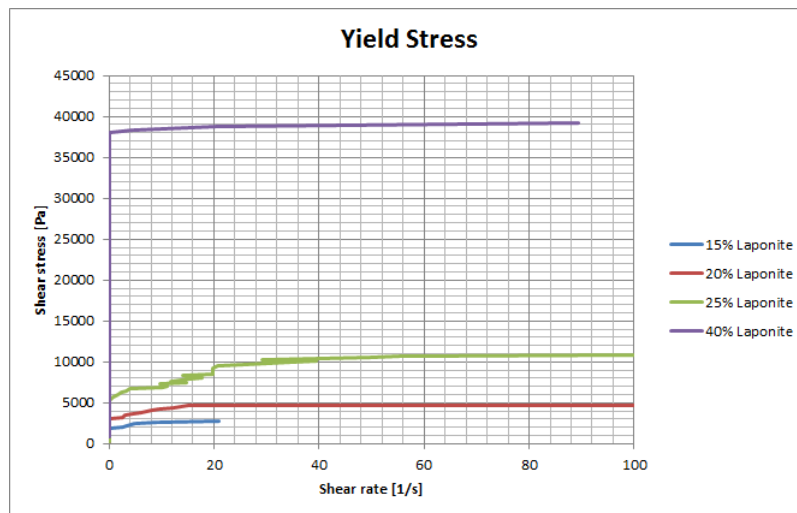


Figure 4.2: Yield stress measurement for different concentrations of laponite in water

A rough correlation between the level of the yield stress and the concentration is that adding an additional 5% of laponite to water the yield stress doubles. For the purpose of the experiment it is assumed that a equilibrium of forces is present, as stated in equation A.7.

The viscosity is calculated as function of a shear rate, the data for different types of laponite concentration is displayed in figure 4.3.

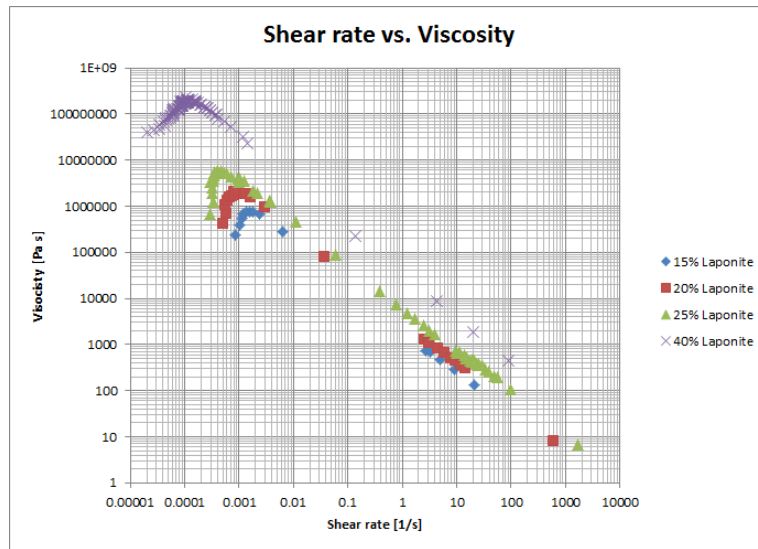


Figure 4.3: Rheology measurement for different concentrations of laponite in water

The graph clearly shows the shear thinning effect of the fluid, in the experiments a mixture containing 20% weight laponite is used.

## 4.2. Swellable Rubber

The study behind the swelling of rubber is called polymer science or macromolecular science [1]. In Appendix A.2.1 a brief introduction is given about swellable rubber and the components that make the rubber swell: a super-absorbent polymer (SAP) or salt. The characteristics for both swell actuators are discussed in this section.

### 4.2.1. Swell Rates

The principle behind a swellable rubber is that the water is absorbed through an osmotic reaction; the water fills the tiny holes which are left by the SAP/salt that move through the solution. The rate with which the SAP [4] or salt move to the solution with a lower concentration is important for the swell rate of the rubber. Experiments in the lab have been conducted with a block of rubber submerged in water of 20 °C, the change in height is measured over time and the data is displayed in figure 4.4.

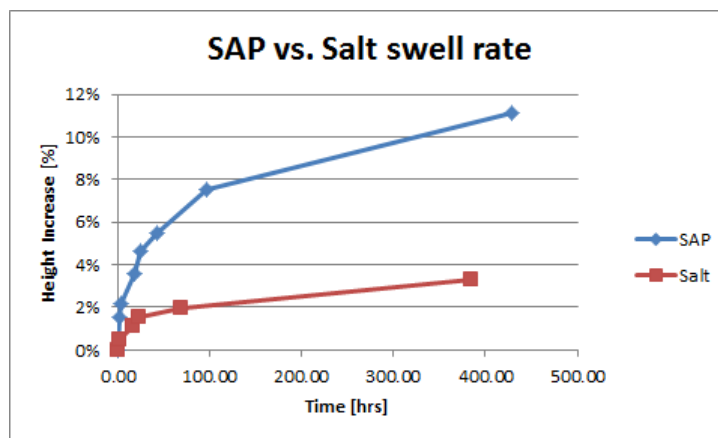


Figure 4.4: Measurements on swell behaviour of SAP and salt rubber in water at 20 °C

### 4.2.2. Final Design

For practical reasons the decision was made to go for a rubber with SAP, since it has a higher swell rate. Experiments in the lab show that under higher temperature the swell rate is higher, yet the experimental set-up was not designed and certified to work with high temperatures. A housing for the rubber is made, with 4 chambers of 5 mm in height and 100 mm in length, see figure 4.5.

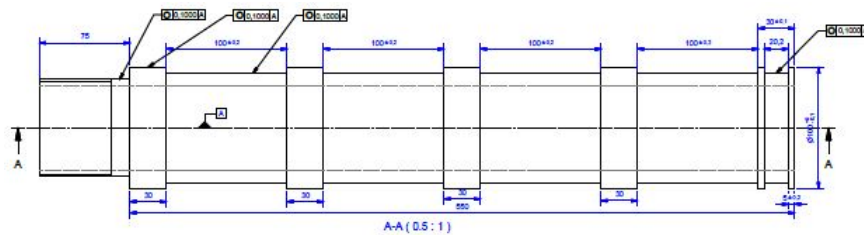


Figure 4.5: Design of rubber sealing ends for experimental set-up

The rubber that will be used is a two compound that cures at room temperature. During the mixing of the two components the SAP will be added and the rubber will be poured into a mold, as displayed in figure 4.6. The OD of the rubber will be 100 mm.

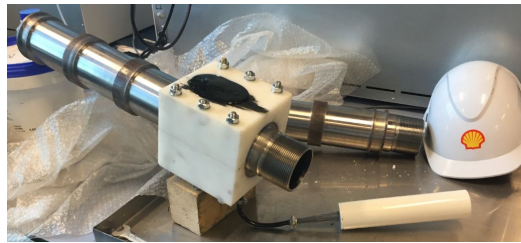


Figure 4.6: Pouring of rubber in mold

## 4.3. Compression Packing

Contrary to the concepts above, compression packing is not designed in-house. Because it is a very straightforward concept, a company has been brought in to help design this concept. Together with the company, Garlock, the issues with design have been discussed and they proposed a specific type of material for the compression packing.

### 4.3.1. Final Design

The OD for the packing is chosen at 4" or 101.6 mm, due to the limitations in geometry the height of the packing is chosen at 6.35 mm. As stated in Appendix A.1.2, a total of 5 packing rings will be installed. More rings will not contribute directly to the sealing pressure. The housing is displayed in figure 4.7.

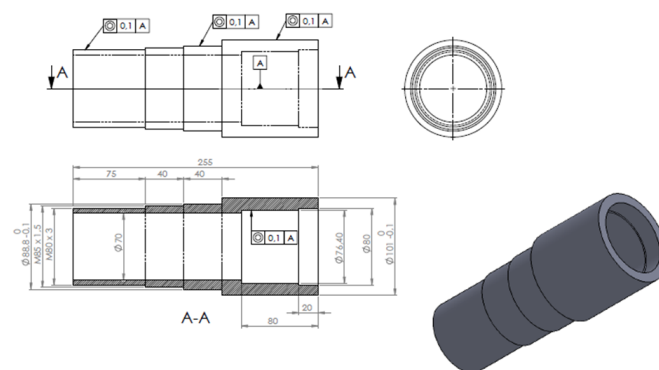


Figure 4.7: Design of packing housing

On both ends of the packing housing threaded connections are made, to be able to connect them to the experimental set-up. The compression force on the packing is supplied by a nut, by applying a torque moment on the nut. The supplier advised to install the compression packing with a sealing of pressure of twice the pressure of the medium. This corresponds to a required torque of approximately 3.5 kNm.

The rings are positioned in such a way that the open ends are always more than 90 °apart in circumferential direction, as displayed in figure 4.8. The ends are cut at an angle of 45 °, to ensure pressure is transferred from one ring to another.



Figure 4.8: Installation of packing rings on housing

## 4.4. Chevron/V-Packing

Like the compression packing, the chevron/v-packing are designed by Garlock. For ease of use the same design for housing and compression of the seal is used as described in section 4.3.1 and figure 4.7.

### 4.4.1. Final Design

The final design of the chevron seal consists of 5 V-rings, an actuator ring and a back-up ring, see figure 4.9. Both chevron seals are mounted with the actuator ring facing the pressure side. This way with increasing pressure in the chamber, the actuator ring is compressed further and the V-rings are pressed harder to the SOCCS casing.



Figure 4.9: Design of Chevron set

The required compression force for the chevron seal is equal to the medium pressure, so a torque force of approximately 2 kNm is required to compress the chevron set.



# 5

## Results & Discussion

The data obtained through full scale experimental testing is discussed in this chapter. For every concept the required preparations for the test are explained in more detail with the corresponding observations. Afterwards the results from the tests will be qualitatively discussed in more detail, with the ultimate goal to understand more on the physical principles at work. The chapter is divided into 4 sections:

1. Non-Newtonian Yield Stress Plug (section 5.1)
2. Swellable Rubber (section 5.2)
3. Packing Seal (section 5.3)
4. Chevron Seal (section 5.4)

Since the last 2 concepts have been manufactured by a company, the results of these tests will limit to analyzing the data and visual observations during testing.

### 5.1. Non-Newtonian Yield Stress Plug

The initial experiment was performed with a mixtures containing 40% laponite, during start-up of the full scale test the mixture clogged the flow tubes in the set-up. This was due to the settling of the particles in the fluid, this was solved by using a high shear mixer, which counters the settling of the laponite particles. To not risk clogging the entire set-up again the decision was made to begin testing with a mixture containing 20% laponite.

#### 5.1.1. Test Results

Because the success of this concept relied on the properties of the mixture, certain steps had to be tested to confirm that the fluid had the same properties as in the lab scale experiments. Checks have been performed to be certain of the properties of the fluid in the set-up, the collected mixtures have been placed under the Rheometer again. The conclusion was that the rheology properties were equal to the properties of the mixtures in the lab scale experiments. A visualization of the mixture used in the set-up is displayed in figure 5.1.



Figure 5.1: 20% laponite mixture after precipitation reaction in set-up

Both sealing ends consisted of pipes with an OD of 100 mm and a length of 800 mm. The results for the static test are shown in figure 5.2.

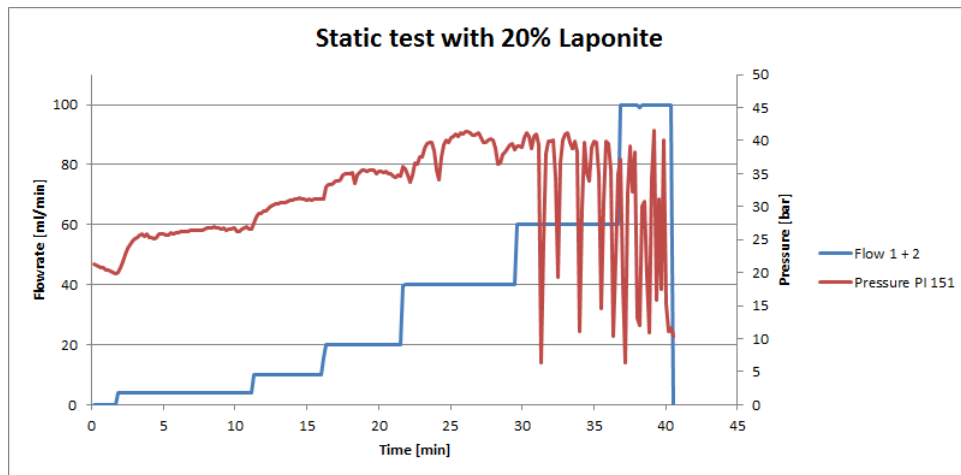


Figure 5.2: Static test of 20% laponite mixture

The test have been performed using an open-loop system, meaning that the only the flow rate is controlled and the resulting pressure is measured. The flow rate is increased stepwise, to a maximum of 100 ml/min. The figure shows that as the flow rate increase the resulting pressure does not increase proportionally. Apparently above a certain flow rate or pressure the system becomes unstable, thus the measured pressure is not constant any more, in section 5.1.2 possible causes for this phenomenon are described. Elasticity in the system is not the cause of this instability, since the test is performed in an open-loop system. A dynamic test with the same fluid is also performed, results are displayed in figure 5.3.

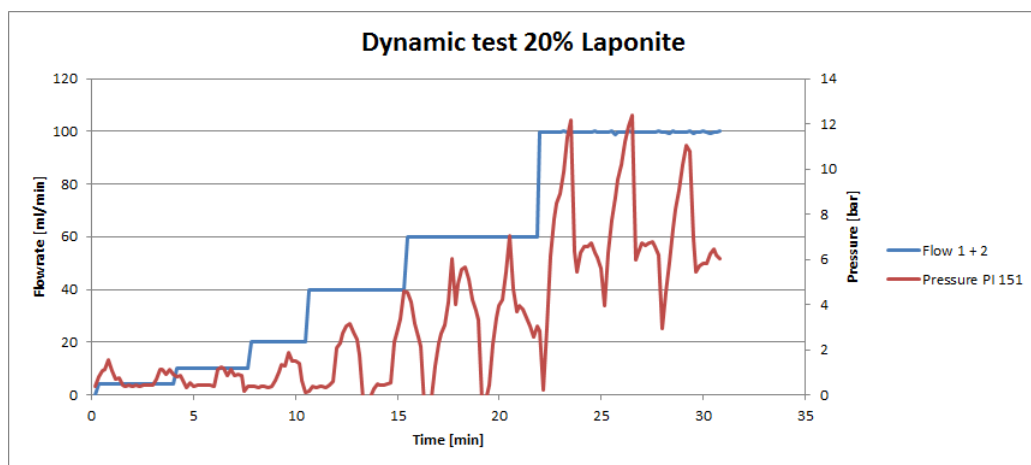


Figure 5.3: Dynamic test of 20% laponite mixture

As in figure 5.2 the system is also put in open-loop mode, thus the flow rate is increased with steps. If the data of the two figures is analyzed, it is clear that during dynamic behavior the pressure levels are much lower. This is understandable since the movement of the SOCCS casing creates an ever higher shear rate at the contact area with the fluid, thus lowering the viscosity and a higher flow rate is necessary to reach the same pressure. The pressure in the figure also shows a repeating trend, this is due to the reciprocating movement of the SOCCS casing. A single phase corresponds to 1 stroke back and forth of the casing.

### 5.1.2. Instability

The instability observed during the static experiment can be triggered by multiple events. This section will shortly discuss different theories, which could be the cause of the instability. First it is important to zoom in on the instability in static conditions, this is done in figure 5.4.

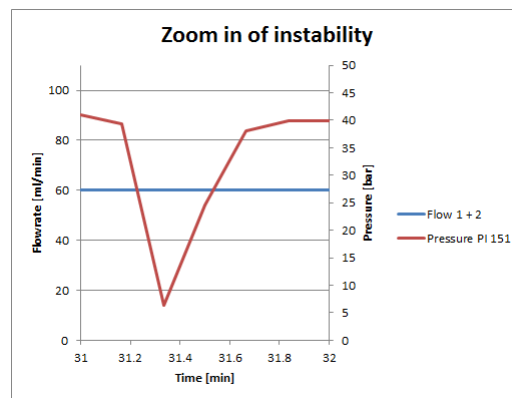


Figure 5.4: Close up look of instability from static test with 20% laponite mixture in open-loop system

The sampling rate during the test was every 10 seconds and a single instability occurred in around 20-30 seconds. In order to better describe the instability it is necessary to repeat the test at a higher sampling rate, preferably less than 1 second per data point. The rest of the drops in pressure according to figure 5.2 have a similar profile as the one displayed in figure 5.4.

1. An explanation of this phenomenon is that the fluid displays visco-elastic behavior [11], making the properties of the fluid not only dependent on the shear rate but also on time. This assumption backed up by the fact that at high flow rates the fluid displays a less viscous structure than at low flow rate, yet this is only based on visual material and has to be confirmed by more tests. In this situation the laponite recovers from undergoing high shear rate, as in the static mixer during the experiment.
2. A follow-up theory from the one described above is a Rayleigh-Taylor instability, which happens between the interface of two fluids having different viscosities. In the experiment there are not directly two different fluids, but in combination with the history effect of the laponite this could be achieved. Still a Rayleigh-Taylor instability would most likely occur at high flow rates and low viscosities, so this theory is abandoned as well.
3. Stick slip motion of the fluid could also be a possible cause behind the instability. But this theory does not hold up why the pressure recovers after a drop.
4. The possibility of going from a laminar to turbulent region is also not very likely. Because the viscosity of the mixture is very high the Reynolds numbers are extremely low, thus shifting to the turbulent flow regime is not expected. Furthermore this theory also not explains the recovery of pressure.
5. The theories above all presume the instability is triggered by a flow related issue, it is also possible that the instability is caused by reaching a critical pressure. Normally water is only compressible at very high pressures and the compressibility of water is not more than 1-2%. But a mixture containing this high percentages of laponite cannot be entirely characterized as fluid. In the mixture the laponite discs form a solid card-like structure, with water between openings of the discs. In a closed surrounding the card-like structure would not deform if pressurized, since the water would exert the pressure in all direction homogeneously. But in the case when the fluid subjected to a pressure gradient it is possible that the card-like structure would change shape, because a pressure difference on a solid object can trigger deformations.

Looking at the possible theories above the last theory mentioned is the only one that is capable of explaining the recovery of pressure after a drop. This theory is triggered by the compacting of the laponite molecules in the card-like structure, during this compaction the system is able to build up pressure. But eventually this exceeds a certain limit and the structure fails, resulting in a drop of pressure. Afterwards it is possible again for the fluid to form a structure again and thus the instability continuous. To examine this behaviour further it is necessary to look into the micro molecular structure of the laponite molecules. It could be possible to test this by pressurizing laponite in a cylinder and measure if there is any volume decrease. Dielectric spectroscopy is also a possibility to measure the dielectric properties of a medium.

### 5.1.3. Model comparison with experiments

The CFD simulation is performed for the different flow rates to compare with the obtained data through experiments, the results is plotted in figure 5.5. Appendix D gives an overview how the CFD model is build up and which assumptions are made.

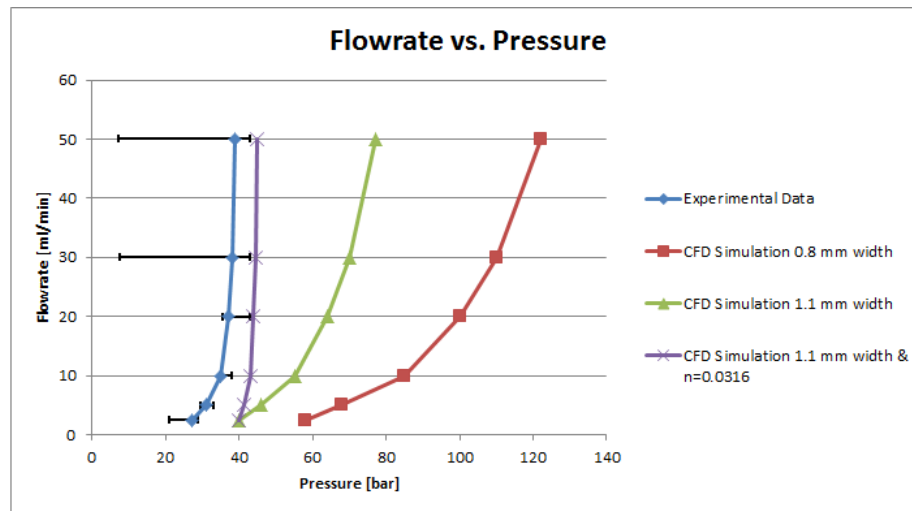


Figure 5.5: Comparison of experimental data with CFD simulations in static conditions

Error bars have been added to the data points for the experimental data, which show the lowest and the highest flow rate during testing. The error bars corresponding to a flow rate of 30 and 50 ml/min are rather big compared to the rest; this is due to the unstable effect observed during the experiment. The different CFD simulations are explained below:

1. CFD Simulation 0.8 mm, corresponding to the red line, is the basic output of the CFD model as described in section D.1.1. The acquired values are much higher than measured during testing, this is as expected, since factor as eccentricity and out of roundness are not taken into account.
2. CFD Simulation 1.1 mm, corresponds to the green line, is done because from figure 3.1 it is clearly visible that a axisymmetric gap of 0.8 mm does not relate to reality. Therefore a bigger gap of 1.1 mm is chosen, the results is that the line shifts more towards the values from the experiments. Apart from the decrease in absolute value the curve of the data points also is less, thus representing a higher shear thinning effect with a bigger gap. This observation is correct since the regions in which the velocity gradient is close to "0" is wider, see figure D.3 and therefore contributes less to the pressure gradient over the length of the gap.
3. In CFD Simulation 1.1 mm width &  $n=0.0316$ , the purple line, not only has the width of the gap changed but also the rheology properties of the fluid have been altered. This clearly does little to the lowest absolute value compared to the green data points, but it has a big influence on the curve of the data points. The fluid properties are calculated through the fitting rheology properties of the fluid with the Rheometer, this is further discussed in section 5.1.4.

It can be concluded that using a CFD simulation programme is capable of predicting, to a certain extent, the outcome of an static experiment in which a mixture of water and laponite as a Non-Newtonian fluid is used. Yet the CFD simulation does not explain the unstable behavior of the fluid at high pressure, the advice is to further investigate the cause of this instability and see if it is capable to implement it in CFD.

Apart from the static condition the CFD simulation in Appendix D also showed that it is not possible to build up pressure when the SOCCS casing is moving in line with the laponite. This behavior corresponds to the test results from figure 5.3, because the pressure sensor is mounted at the beginning of a seal it also detects the pressure drop. The pressure drop and gain correspond to the direction of movement of the SOCCS casing. This shows CFD is also an applicable tool for dynamic conditions, yet the same problems concerning instability at high pressure could be present.

### 5.1.4. Data Fitting

A big influence in the outcome of the CFD simulation is the way in which the fluid properties of the mixtures are characterized by a fitting curve. The data points are retrieved from measurements in the Rheometer with a cone and plate set-up. A problem that arises during the measurement is the extrusion of fluid from under the cone, therefore the normal force on the fluid drops and this could possibly lead to differences in measured data. This is prevented with putting the cone in a cylinder shape to minimize the gap in which fluid can extrude from the sample, as shown in figure 5.6. During the measurement it is necessary to keep the cylinder in place, this is done by hand. So it is not very certain the results from these measurements are very accurate, the mixture is simply pushing the boundaries of the measuring equipment.



Figure 5.6: Prevention of extrusion of fluid during measurement

Multiple theories have been derived for curve fitting of Non-Newtonian fluids, all possible theories are displayed in figure 5.7. The CFD model is only capable of using a Power-Law & Bingham fitting methods for Non-Newtonian fluids, while in real life the mixture of laponite and water is more related to a Herschel-Buckley fitting method.

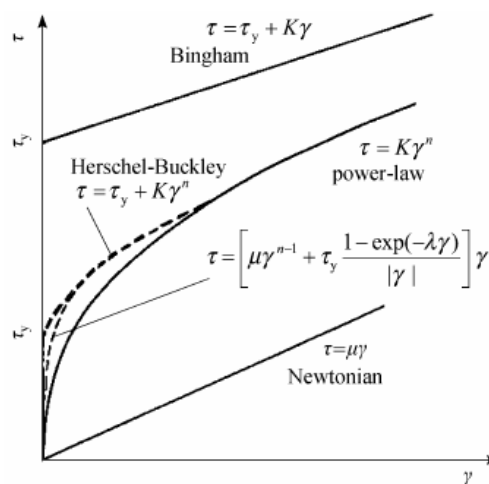


Figure 5.7: Different methods of data fitting

The first two methods have been used to fit the data of a 20% laponite mixture, as seen in figure 5.8. The fluid clearly shows some strange behavior, since there is a sudden drop at a certain shear rate. The figure clearly shows both curve fitting methods are not accurate.

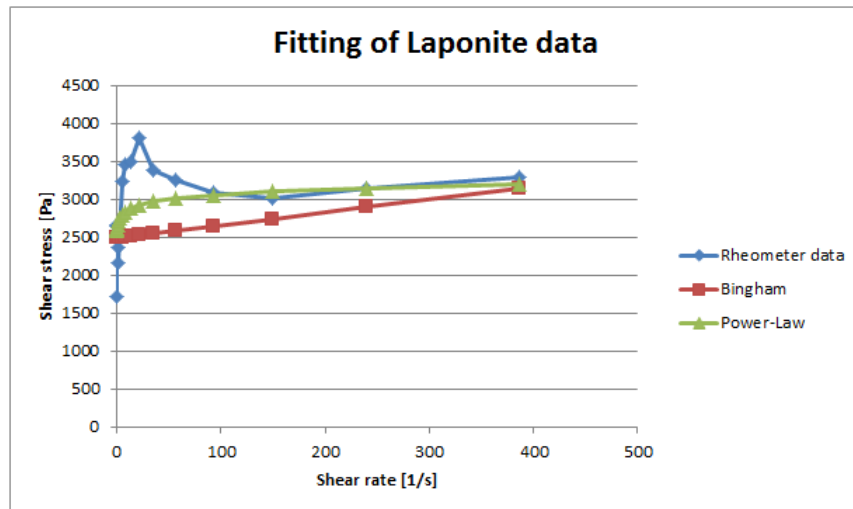


Figure 5.8: Fitting of obtained data of rheometer measurement

As mentioned in the beginning of this section the measuring of a high concentration laponite mixture is very difficult and pushing the measuring device to its limits. Even with a special containment cylinder around the cone it is still expected that there are large errors during measuring. It would be better to test the fluid under a constant pressure.

Thus far it is possible to conclude that data fitting has a large influence on the characterizing of the laponite fluid and therefore on the output of the CFD simulations. Further investigation is necessary to obtain good rheology properties from the fluid.

### 5.1.5. Discussion

In order to proceed with this concept it would first be necessary design two additional small scale set-ups in which both the deformation of the card-like structure as the more accurate measuring of rheology properties is possible. At this point the CFD simulation shows some promising results that it can be used as an estimate for experiments and it is therefore possible to find a solution through this road. But the fundamental aspect of the instability has to be determined first. Secondly is that the outcome of the CFD simulation is greatly depended on the input values of the rheology properties, because the measuring of the data is still subject to discussion this problem also needs to be addressed in further research.

## 5.2. Swellable Rubber

The initial experiment was tested according to the final design as in section 4.2.2, one chamber with a length of 100 mm and an OD of 100 mm in length was filled with the compound, see figure 4.6. The seals were inserted in the SOCCS casing and the SOCCS casing was flooded with water to enable the seal to swell.

### 5.2.1. Test Results

According to the data on the swell rate of the seal it is expected for the seal to completely swell against the SOCCS casing, or in other words achieve 10% increase in height, after approximately 2 weeks, see figure 4.4. During these 2 weeks some static test were performed to see if the seal would hold any pressure. Apart from static test dynamic test were also performed to see what the magnitude of the friction would be, in case the friction would come to close to the maximum pulling force of 5 tons of the experimental set-up.

The static tests showed no increase in pressure at maximum flow rates and therefore after 2 weeks the seal were pulled out of the SOCCS casing to measure the increase in diameter. In figure 5.9 the increase in the height of the seal in the full scale experiment is plotted against the increase in the lab scale experiment.

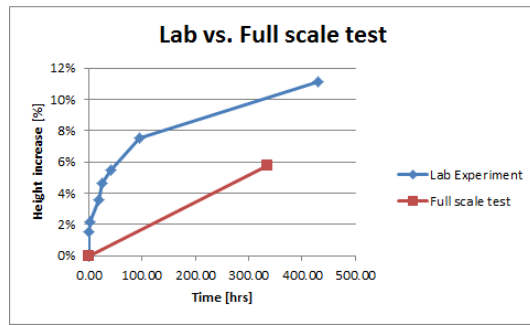


Figure 5.9: Percentage of height increase in full scale set-up vs. lab experiment

From this figure it is clearly visible the rubber in the full scale test swelled much slower than in the lab experiment. This was in the line of expectation, since the flooding of the SOCCS casing gave some trouble, so it could well be that the seal was not always in contact with water. Another interesting fact was that the rubber exhibited a so-called bleeding effect, or the accumulation of polymers on top of the rubber. This creates a very viscous layer of gel on the outside of the rubber, see figure 5.10.



Figure 5.10: Results of bleeding of polymers out of rubber

Since the principle of a water swellable rubber is based on an osmotic pressure, a thick layer of polymer and water mixture on top of the rubber will change the osmotic pressure in equation A.1. The gel will decrease the solubility of the polymer still trapped in the rubber with the water, there for the molarity from equation A.2 will decrease. Consequently the rubber will swell less quick and therefore the first test is considered failure. A second test was performed where the initial OD of the seal was increased to 101 mm. During the test the seal was also removed from the SOCCS casing and the layer of gel was removed from the seal to keep the interaction with water as good as possible. After two weeks a static test was performed with an open-loop controlled process [16]. The input was controlled flow rate (CF) of the pumps and the pressure was measured, as displayed in figure 5.11.

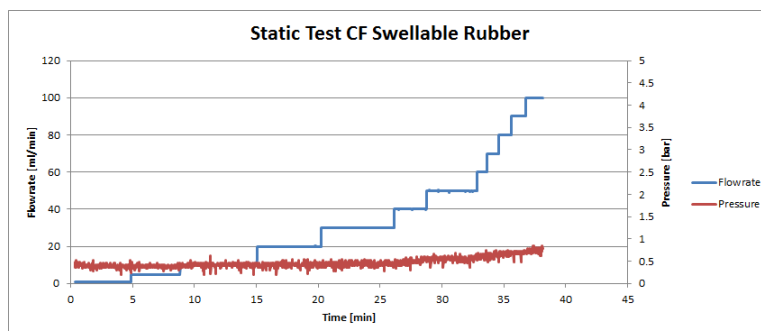


Figure 5.11: Static Test of swellable rubber with an open-loop system

Before the test commenced a measurement of the OD of the seals was taken, the seals had an average OD of 102.1 mm. Yet the test showed the seal was still not able to hold any significant pressure at the maximum flow rate. If the measured OD from the seal is compared to profile in circumference of the SOCCS casing the result is logical. Figure 3.1 shows that with an OD of 102.1 mm, or approximately a radius of 51 mm, the seal would still not touch the top of the SOCCS casing were the weld is located. In this section a gap still remains of around 0.3 mm, through which the water flows and is not able to build of pressure. A dynamic test has also been done to look at the reaction force due to the friction of the rubber seal with the SOCCS casing. Figure 5.12 shows that the reaction force already had a magnitude of 20 kN, this was more than originally was anticipated.

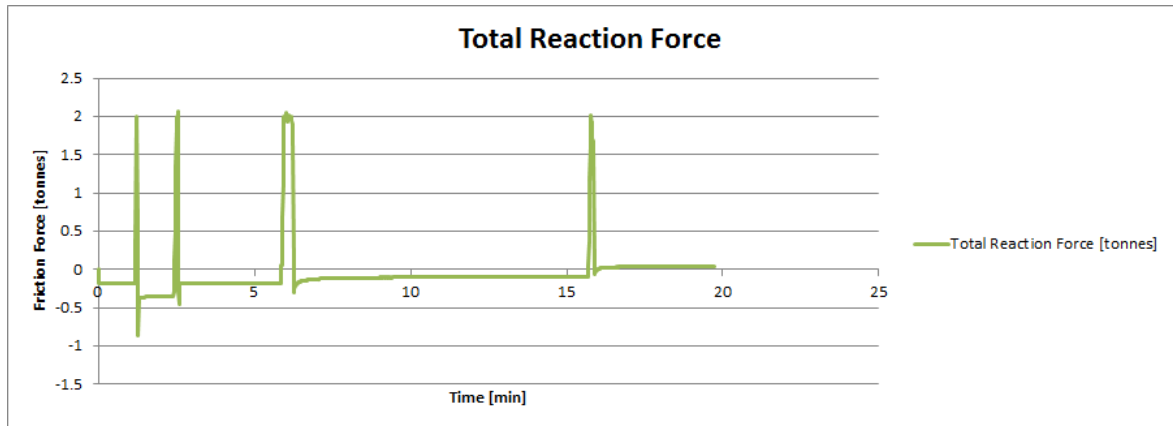


Figure 5.12: Pull out test of seal

During the test the motor came close to the maximum torque it could deliver in this operation, for safety the maximum torque had been lowered, corresponding to a pulling force of 2.5 tonnes. After multiple tries to pull the seal free the system finally overcame the static friction, afterwards the dynamic friction was much lower as displayed in figure 5.13.

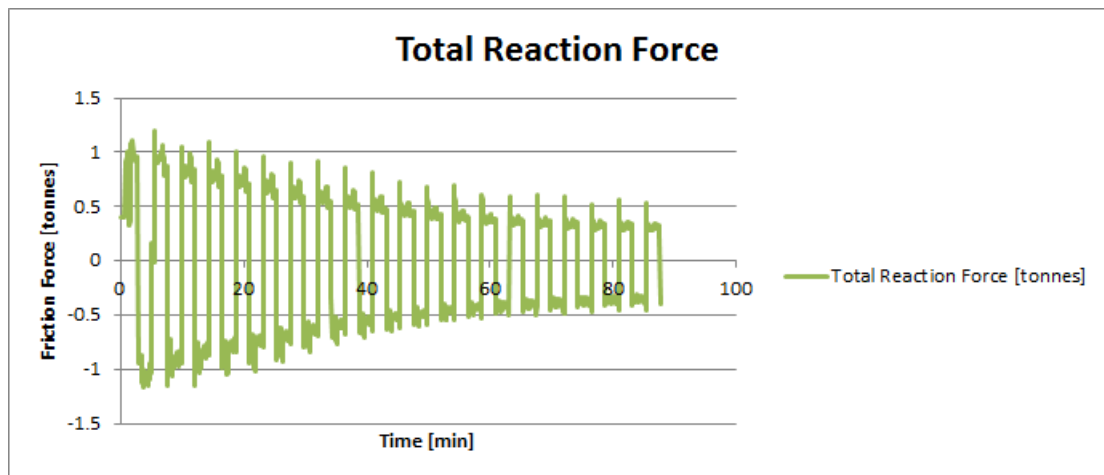


Figure 5.13: Measurement of dynamic reaction force of swellable rubber with a open-loop system

Because the friction of the seal was already very high, it was decided to cancel the experiment for risk of jamming.

### 5.2.2. Discussion

Since both tests were not even able to perform as suspected it not possible to say if a water swellable rubber would work in principle, however for this application a water swellable rubber is not practical, namely due to the slow swelling rate. However it is fair to say that they are not practical, namely due to the slow swelling rate. Another important issue is that the friction force of the rubber is very high, if the seal would be swollen

to the SOCCS casing it would only increase the required friction force. Below a list of the lessons learned and suggestion for further development:

- Use a rubber with SAP instead of salt, this will speed up the swelling rate.
- Start with a smaller length of seal, in order to decrease the friction force.
- If possible use water at a higher temperature, to increase swelling rate.
- Make the OD of the seal as large as possible, so that the initial gap with the SOCCS is as small as possible.
- Try to increase the viscosity of the water, in order for the fluid to act as a lubrication to decrease the friction.

### 5.2.3. Oil Swellable Rubber

Instead of finding a viscous water-based fluid in which the rubber still swells, it is also possible to use an oil-based swellable rubber. The principle behind swelling in oil is different; swelling in oil is based on the dissolving of the rubber into oil. The long polymer chain in a rubber want to solve in oil and basically pulled towards the oil, thus an increase in volume is achieved. A downside of this is that the material properties of the rubber change, due to swelling the rubber gets softer.

Dissolving is based on the solubility parameter of both the liquid and the elastomer. When the solubility parameters of two materials are close, they dissolve into each other to even the concentration throughout the mixture. Solubility is predicted by the Hildebrand index, the Hildebrand's solubility parameter [6] is the square root of the cohesion energy density, see 5.1.

$$\delta = \sqrt{\frac{\Delta H_v - R_{gas}T}{V_m}} \quad (5.1)$$

Small scale lab experiments have been performed to look at the rate of swelling of different types of rubber and different types of oil-based fluids. The results are displayed in figure 5.14.

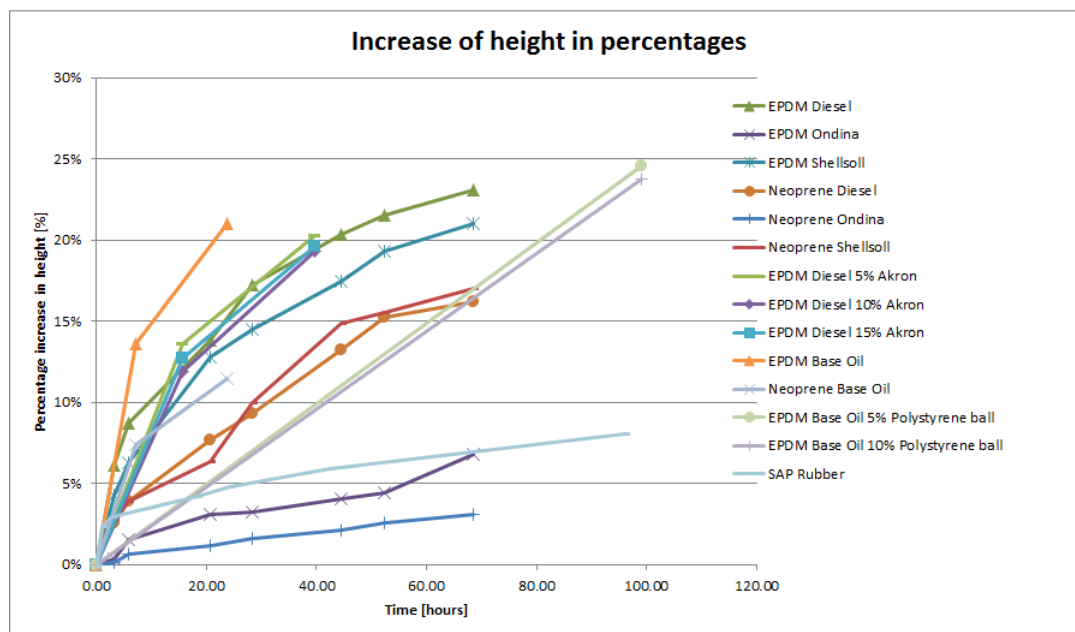


Figure 5.14: Percentage of height increase of rubbers in oil-based fluids

The figure clearly shows that a rubber swells much faster in an oil-based fluid than a water-based fluid. A Base Oil has the most potential and is also beneficial in practice, since it is a basic component of most drilling fluids. Additives are used to give different rheology characteristics to the fluid, and make the fluid more viscous. The effects of the different additives on the rheology properties is displayed in figure 5.15.

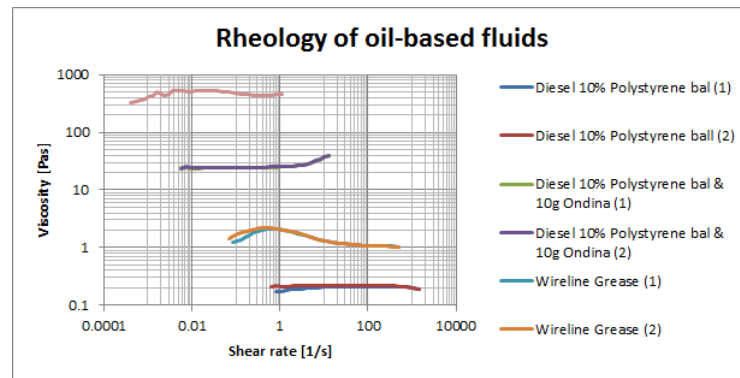


Figure 5.15: Rheology properties of oil-based fluids vs. water-based fluids

Compared to the water-based mixtures of laponite, the oil-based fluids have a few beneficial rheology properties. Firstly the behavior seems to be rather as a Newtonian fluid, meaning that the viscosity is constant for every shear rate. This would make the outcome of a full scale experiment more predictable, since the concept would behave more as the original Hagen-Poiseuille equations. Secondly there is still a fair amount of control over the viscosity of the fluid, because the original idea was to recreate a fluid that is used in wireline operations. Which has an average viscosity of about  $1 \text{ Pa} \cdot \text{s}$ , yet lab experiments showed that it is possible to achieve a viscosity which is about 400 times more viscous.

A downside of using an oil-based swellable is the change in material properties, since the used EPDM rubber went down in hardness from 75 Dura to 45 Dura. This would increase the change of extruding the rubber from its housing during testing. Yet further development of this concept is recommended, especially because the oil-based fluid can also be used in combination with different concepts. Even concepts that do not need a swellable rubber can still benefit from the good rheology properties of the base oil.

### 5.3. Compression Packing

As mentioned in section 4.3 the compression packing is tested in a single configuration, one consisting of a graphite material is used. Variations in compression force and fluid are also tested.

#### 5.3.1. Test Results

Test with water

The first test consisted of the packing to be tested in static condition with water. The first tests showed that the packing needed to be compressed hard against the SOCCS casing, no torque wrench was possible to measure the required force. The results of the first test are displayed in figure 5.16. The process was pressure controlled by the pumps, so once a pressure was given as an input to the pumps the system tried to regulate at that pressure altering the flow rate. The regulation is done by a proportional integral derivative (PID) controller. The downside of using a pressure controlled system, opposite from using an open-loop or flow controlled system, is that elasticity is introduced. The system will always need to correct itself and thus this need to be taken into account when analyzing the data.

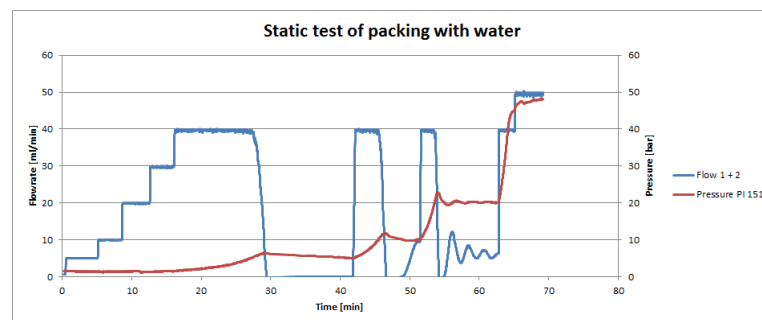


Figure 5.16: Static test of packing seal with water in an open-loop system

The observations during testing and the input of the system is mentioned in the table below:

Table 5.1: Observations and control settings during testing

Time [min]	Control Settings	Observations
$t_0$	CP at 5 bar at pump flow rate of 5 ml/min No movement	-
$0 < t < 40$	flow rate is increased with steps to 40 ml/min.	After a while, at a flow rate of 40 ml/min, pressure gradually builds up. At around $t = 30 \text{ min}$ the set pressure of 5 bar is reached and the system regulates the flow to maintain it at that level, which is close to almost 0. Apparently a minimum flow rate is necessary to activate the sealing mechanism of the packing seals, applying extra compression force on the packing seal.
$40 < t < 45$	Set pressure is increased to 10 bar.	System responds by increasing the flow rate to the maximum of 40 ml/min.
$45 < t < 65$	Set pressure is increased to 20 bar.	Again system pumps at the maximum flow rate of 40 ml/min, resulting in an increase in pressure. When the set pressure is reached the system regulates again, the first amplitude in flow rate is registered here and thus the pressure also exhibits an oscillatory behavior. This is due to elasticity in the system induced by the PID controller.
$65 < t < t_{end}$	Set pressure is increased to 50 bar and maximum flow rate to 50 ml/min.	These settings correspond with an open-loop system, because the maximum pressure is reached below the set pressure, thus the system pumps with the maximum flow rate. The maximum pressure the system can hold is around 48-49 bar, there is still a gradually increase in pressure. But due to limitations in fluid the test had to be stopped.

After the static test the dynamic test was performed and the results for that test are displayed in figure 5.17.

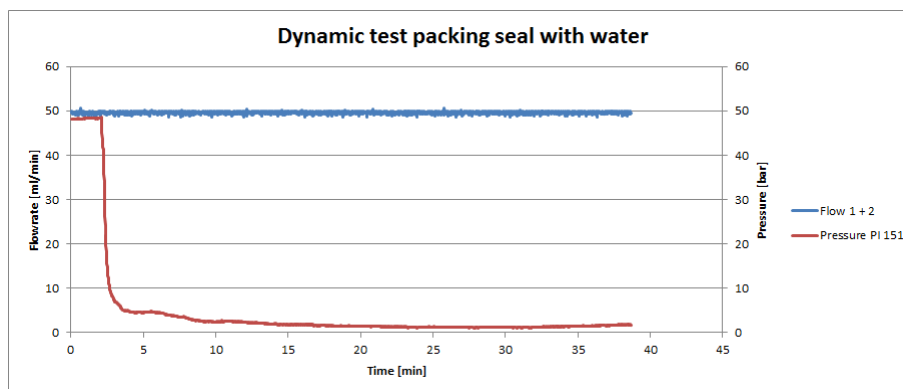


Figure 5.17: Dynamic test of packing seal with water in an open-loop system

The data clearly indicates the compression packing is not able to hold pressure during movement of the SOCCS casing. The pressure stabilizes around 1-2 bar. The test was stopped and the seals were pulled out of the SOCCS casing for inspection, the results is shown in figure 5.18.



Figure 5.18: Deformation of packing seal due to moving of SOCCS casing

Figure shows the packing material is extruded through the gap between the housing and the SOCCS casing. Angular deformation is present in the top part of the material, which reaches out of the housing. Due to the angular deformation the packing seal loses its contact pressure with the housing and the gap between the packing and SOCCS casing gets larger, therefore the seal is unable to hold the pressure. This loss of material, due damage of the seal, is only generated over a distance of 24 m, while in reality the seal should be wear resistant for over 4 km. The figure also displays the position of the weld of the SOCCS casing. Evidently there is no cut, as was expected, but rather the material bended around the weld.

To overcome the static friction force, a pulling force of around 5 kN was required. The dynamic friction force was on average 3 kN.

#### Test with wireline fluid

The second test is performed with wireline fluid instead of water. Additionally anti-extrusion rings have been put in place next to the packing material, to prevent the packing material to deform and extrude out of the housing. The anti-extrusion rings are made from Polyoxymethylene (POM), with a hardness of 85 Dura, installed as in figure 5.19.

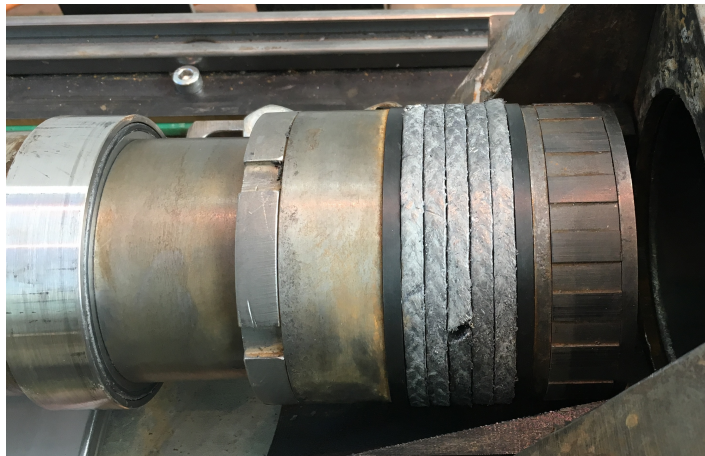


Figure 5.19: Positioning of anti-extrusion rings

This test is performed with wireline fluid, with rheology properties as shown in figure 5.15, which as a somewhat constant viscosity of 1000 cP. It is expected that this increase in viscosity will greatly benefit the performance of the concepts. Since the more viscous fluid will be able to compress the packing rings better than water. Some initial static test showed the packing seal was capable of holding a pressure greater than 200 bar, in CF mode. Due to safety reasons the dynamic test was done in CP mode, the results for the dynamic test are shown in figure 5.20.

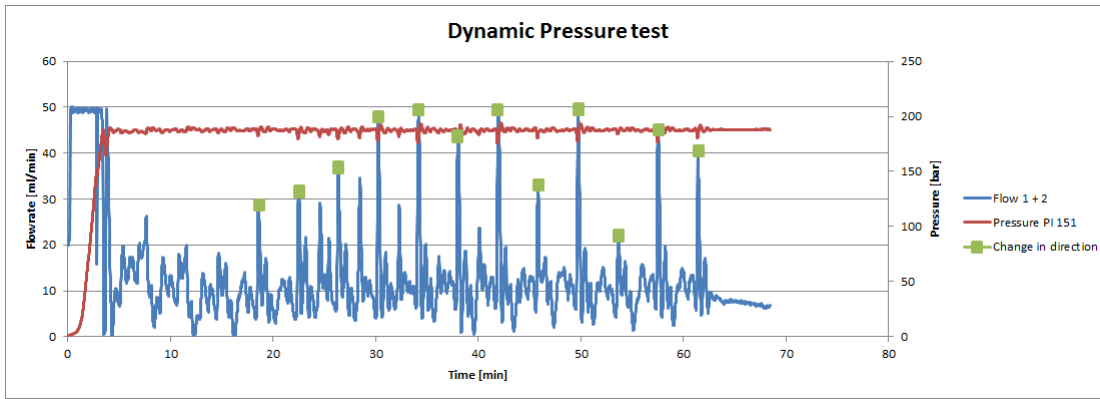


Figure 5.20: Dynamic test of packing seal with wireline fluid in CP mode

The observations during testing and the input of the system is mentioned in the table below:

Table 5.2: Observations and control settings during testing

Time [min]	Control Settings	Observations
$t_0$	CP at 200 bar at pump flow rate of 50 ml/min Movement of 1 m/min	-
$0 < t < 5$	Initial control settings	A rapid increase in pressure is observed, the viscous fluid directly compresses the packing. When the set pressure is reached at around $t = 5 \text{ min}$ the system decreases the flow rate.
$5 < t < 18$	Initial control settings	The flow rate seems to be stabilising around 10 ml/min.
$18 < t < 63$	Initial control settings	Some peaks in flow rate occur in a somewhat constant interval of around 4 min. Leaks are also monitored at the pump and the piston cylinder.
$63 < t < t_{end}$	Movement is stopped	flow rate stabilises at around 7-8 ml/min, with a very large decrease in scatter. The leakage of water is estimated at around 3-4 ml/min, so the actual leakage over both seals is around 4/ ml/min in static condition.

After scanning through the data it became clear that the peaks in the flow rate are a results of the change in direction of the moving SOCCS casing, visualized by the green dots in figure 5.20. Which results in a pressure drop of a few bars, because the PID controller of the pump is programmed to react with a high gain the flow rate is quickly boosted to its maximum. The resulting friction of the compression packing is displayed in figure 5.21.

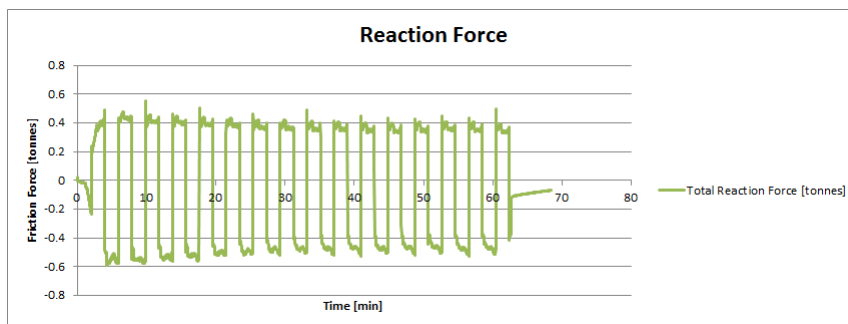


Figure 5.21: Resulting reaction force due to movement of SOCCS casing

An average friction force of 4 kN is observed during movement of the SOCCS casing. The test consisted of 32 strokes, corresponding to a total covered distance of 64 m. Figure 5.21 shows a small decrease in friction overtime, most likely due to extrusion of packing material subsequently losing initial contact pressure. This decrease in reaction force seems to be rather small, but additional test with >1000 strokes should be performed to be sure wear is not an issue. Visual observation of the used seal was also done after testing, the result is displayed in figure 5.22. Due to the higher pressure during the test, the deformation due to the weld is much better visible than in figure 5.18.

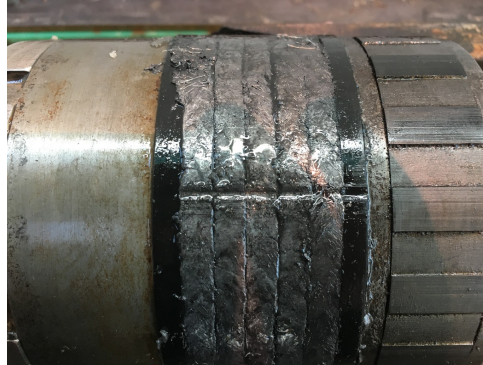


Figure 5.22: Visual observation of seal after testing

### 5.3.2. Discussion

The second test with the wireline fluid clearly performed better than the test with water; a one on one comparison to measure the effect of the increase in viscosity is not possible, since in the second test also anti-extrusion rings were used. Still the combination proved to be within the operational requirements set in table 3.3. With the note that it is still required to perform a test with >1000 strokes to confirm does not become a problem during operations.

The effect of the anti-extrusion rings contributes most during the movement of the SOCCS casing, in comparison with figure 5.18 there is much less material extruded out of the housing in 5.22. This explains the large pressure drop during testing with water, in which the seal was almost not even possible to hold any pressure. Figure 5.22 also shows that the seal is kept more intact than with no anti-extrusion rings. It is still possible to distinguish the separate packing rings. Some extrusion of packing material is still visible, the positions match at the point in which the SOCCS casing has the smallest diameter, as displayed in figure 3.1. On both sealing ends only the anti-extrusion ring at the downward end of the pressure shows signs of wear, this is due to the fact that these rings are fully compressed by the other rings. Therefore the final anti-extrusion rings deforms according to the Poisson's ratio [10], with  $E = 2.5 \text{ GPa}$ ,  $\sigma = 20 \text{ N/mm}^2$ ,  $d = 101.6 \text{ mm}$  and  $\nu = 0.35$  this yields:

$$\Delta d = -d\nu\epsilon_{axial} = -d\nu\frac{-\sigma}{E} = 0.28 \text{ mm} \quad (5.2)$$

The increase of the viscosity is better noticeable during static test. The test with water achieved a maximum pressure of 47 bar at a flow rate of 50 ml/min, whilst the test with wireline fluid was capable of reaching 200 bar at an average of 10 ml/min. Another clear observation was that with wireline fluid the packing seal immediately build up pressure with a flow rate of 50 ml/min, while during the test with water this increase in pressure was much slower. In order to understand more about the correlation between viscosity and leakage it is important to test with fluids having a different range of viscosities, such as shown in section 5.2.3.

To learn more about wear it is still necessary to perform a test with >1000 strokes. The expectation is that this will not have a very large effect on the performance of the seal, since the friction force is rather low; meaning the contact force with the SOCCS casing is low. Due to the reciprocating movement of the SOCCS casing in the set-up it is also expected that in reality wear will be less, since only a movement in a single direction is present.

The final note for this concept concerns the installation procedures. From industry it is known that most failures of packing seals arise due to mistakes during installation. It is still necessary to reproduce the test and see if the same results are obtained.

## 5.4. Chevron Seal

The chevron seals are tested in the same housing as the packing seals, as discussed in section 4.4.

### 5.4.1. Test Results

2 V-rings Chevron test with water

A problem with the delivery resulted in the wrong chevron seals to arrive, namely a set which consisted of only 2 V-rings. Apart from that the rings were all cut; this was fixed by gluing the rings together. A static test was performed with water, as displayed in figure 5.23.

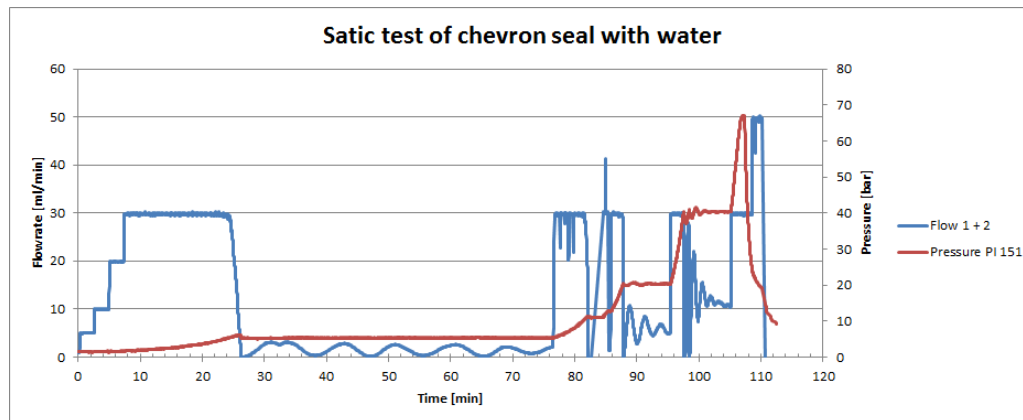


Figure 5.23: Static test of chevron seal with water in CP mode

Input values for PID controller and observation during test are listed in table 5.3

Table 5.3: Observations and control settings during testing

Time [min]	Control Settings	Observations
$t_0$	CP at 5 bar at pump flow rate of 5 ml/min No movement	-
$0 < t < 76$	flow rate is increased with steps to 30 ml/min.	After a while, at a flow rate of 30 ml/min, pressure gradually builds up. At around $t = 28 \text{ min}$ the set pressure of 5 bar is reached and the system regulates the flow to maintain it at that level. Apparently a minimum flow rate is necessary to activate the sealing mechanism of the chevron seals, after which it is possible to build up pressure.
$76 < t < 82$	Set pressure is increased to 10 bar.	System responds by increasing the flow rate to the maximum of 30 ml/min.
$82 < t < 96$	Set pressure is increased to 20 bar.	Again system pumps at the maximum flow rate of 30 ml/min, resulting in an increase in pressure. When the set pressure is reached the system regulates again, it is clear that the amplitude of the regulating flow rate increases compared to the previous section at 5 bar.
$96 < t < 106$	Set pressure is increased to 40 bar.	Same phenomenon as before, amplitude of flow rate necessary to regulate pressure is even larger at this pressure.
$106 < t < t_{end}$	Set pressure is increased to 80 bar.	Pressure increases due to higher flow rate, but at around $t = 107 \text{ min}$ the pressure suddenly drops. An attempt to pump at a flow rate of 50 ml/min does not influence the pressure at all, so the test was stopped.

The expectation was that the seal somehow broke, or that the V-rings were extruded out of the housing. After pulling the seal loose of the SOCCS casing the seal was visually inspected, the result is shown in figure 5.24.



Figure 5.24: Tearing of glued connection due to pressure

The red arrow in the figure indicates the place where the one V-ring was glued together. Apparently the glued connection broke and the V-ring deformed in such a way that the lip was folded. When demounting the chevron seal from its housing another issue came to light, the bottom part of the seal touched the SOCCS casing during entering of the seal in the pipe. The resulting generated friction force was large enough to deform the entire chevron set and twisted it. This effect is showed in figure 5.25.



Figure 5.25: Twisting of chevron set due to contact with bottom of SOCCS casing

Because the data in figure 5.23 displayed an abrupt loss of pressure, the assumption is made that this is due to the broken connection of the V-ring instead of the twisted chevron set. The twisted chevron has been present during the entire static test, and its effect would be more gradually or limit the maximum achievable pressure. Either way the seal did not perform well, due to the design problems. In the original planning a test with a chevrons seal and wireline fluid was incorporated, but due to time limitations this test is not carried out for this thesis.

#### 5.4.2. Discussion

Just as with the packing seal the chevron seal needs a flow rate high enough to activate the sealing mechanism. It is obvious that this required flow rate for activation is lower than with compression packing, because of the shape of the chevron seal is also self-activates by pressing the V-lips to the SOCCS casing. Due to this self-activating mechanism the chevron seal is capable of building up pressure quicker and hold higher pressure than compression packing. A drawback of this sealing mechanism is that the V-lips are exposed to larger deformations, in the end this deformation resulted in tearing of the glued connection evidently destroying the seal.

Testing the chevron seal in combination with the wireline fluid will most likely have the same influences on the results. Activation of the seal will be achieved at a lower flow rate and higher pressure can be achieved. If it will prevent the deformation of the guidance rings due to friction with the bottom of the SOCCS casing is

not expected. This still poses a big challenge for this concept to perform during dynamic test, anti-extrusion rings will have less effect since no material is extruded. It will be more beneficial to design better centralizers, so that the bottom of the seal does not have a high contact force with the SOCCS casing.

Still the first improvement should be to order seals that have not been cut and a set containing 5 V-rings. Using a chevron set with larger dimensions could also improve the performance of the seal. Because re-designing the housing of the seal would take more time and it would exclude the possibility to further test with the wireline fluid it is decided not to incorporate it in this thesis. Due to the quick activation mechanism of the chevron seal it is still advised to perform test with this concept. Because this seal could also be used as an additional seal for holding off a kick. The chevron seal would then be used as an extra redundancy, positioned with the opening towards the well hole as displayed in figure 5.26.

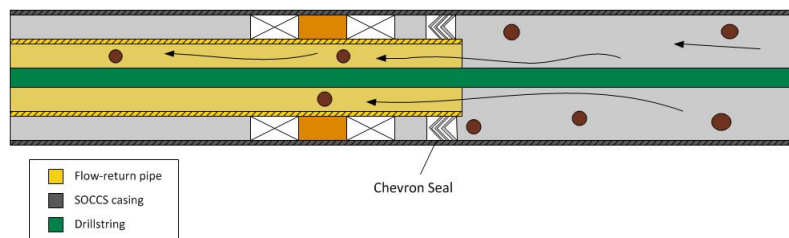


Figure 5.26: Twisting of chevron set due to contact with bottom of SOCCSC casing

In this concept other seals will be present to hold the pressure of the medium, in order to test the welded SOCCS casing. While the chevron seal will only be activated due to pressure from downhole in the well. Because the SOCCS casing moves to the right in figure 5.26 it is not very likely the seal will be twisted or extruded out of the housing.



# 6

## Conclusions

In the past years, Shell has developed a new well construction technology, with that new technology new challenges arise as well. A challenge for the near future is to develop a high pressure dynamic seal. This study presents an overview of possible concepts and discusses the results and phenomena, which are observed when the selected concepts are tested in the designed full-scale experimental set-up.

The first objective of this study was to identify possible concepts that could be implemented in the well construction technology. The methodology used for selecting the most promising concepts has been done based on the ELECTRE method. Additionally the results of this concept selection have been discussed, to confirm the outcome of the selection. Four concepts were chosen to be ready for full scale experimental testing, two of the concepts were designed in-house while the other two concepts were designed in collaboration with an external company. This methodology was perceived as functional, since it required a quick understanding of all different concepts and the emphasis was on the discussion rather than the outcome.

Secondly the goal of the study was to design an experimental set-up, to allow for testing a wide arrange of different concepts previously selected. The design of this set-up has been done with the help of a support team. To be able to test under operational conditions, the decision was made to design with no scaling ratio, thus the set-up was in real scale. The set-up is able to incorporate a range of different concepts, by easily changing out different parts. As space dimensions are limited a system using a reciprocating movement in chosen, to be able to perform long distance tests for wear. The pressure is supplied by 2 pumps with a maximum flowrate of 100 ml/min combined; additionally to the pressure sensors of the pumps two external pressure sensors are installed to measure the pressure in the pressure chamber. The friction is measured as a reaction force on the stinger. The distance is measured by a pulling wire connected to the moving SOCCS casing.

All and all the set-up performed very well and proved to be a precise tool as well as very easy to work with. The measurement devices were adequate and capable of achieving the required accuracy that was necessary. However it would be better in the future to have a better picture of flowrate in the set-up, now it is not possible to know if a seal on one end has less or more leakage then the seal at the other end. Since some seals are not symmetric this is important to know. The elasticity in the system is also an important issue to keep in mind, during the closed loop tests. The settings of the PID controller have a large effect on fluctuating pressure of flowrate and greatly influence the test results. In order to fully decouple the influence of the fluctuations it is necessary to calculate a proportional gain that suits the system.

The third objective of this study was to test and analyse the earlier selected concepts. Tests have shown that the proposed theory for Non-Newtonian Yield Stress Plug is not applicable, due to the shear thinning and time-dependent properties of the fluid analyzing the results qualitative proved to be insufficient. The maximum achieved pressure in dynamic conditions was 10 bar, with a friction force of 4 kN. Therefor the first steps are taken to make a model of this concept and the conclusions from the CFD simulations are:

- It proved to be possible to model the experiments as a Non-Newtonian flow between two parallel plates.
- The model showed a similar behavior as in the tests, it also showed in the dynamic situation in which both the fluid and the SOCCS casing move in the same direction it is not possible to build up pressure.

- The CFD model lacks the possibility of explaining the observed instability at high pressure.
- Both the height of the annular gap and the input parameters for the rheology properties are the biggest influence on the outcome of the model.
- There is still a lot of uncertainty in the data fitting method for laponite. Both the Power-Law as the Bingham models do not fully fit the curves from the laponite data. Obtaining the laponite data also has some issues,

Unstable behaviour is observed at high pressure, most likely due to the deformations in the molecular structure of the laponite discs. In order to further explain this phenomenon it would be interesting to measure the volume decrease of a mixture of water with laponite when pressurized. More information could also be obtained when measuring the medium with dielectric spectroscopy.

The test with swellable rubbers in water not proved to be a success, due to bleeding of the SAP out of the rubber the swelling conditions worsened compared to lab swelling conditions. Thus the rubber was not even able to seal off the gap and the resulting pressure was only 0.5 bar. Even when the seal did not close off the gap, a very high friction force was still observed. A possible alternative is found in using a rubber that swells in oil, the principle behind this swelling is not due to osmotic pressure but to the solving of the rubber into the oil. Not only does this rapidly increase the swelling rate, using an oil-based fluid has most likely also a positive contribution as a lubricant; this could decrease the friction and leakage of this concept. Tests have been performed and it is found that a fluid with base oil as the main component has both good swelling properties and has a promising Newtonian fluid behaviour with a very high viscosity.

Chevron seals proved to be capable of achieving the highest pressure level during the first test. But after achieving a pressure of 67 bar with water in static condition the lips of the chevron seal folded. This is due to the fact that the supplier did not deliver the wright design.

Compression packing proved to hold pressure up to 47 bar in static condition at a flowrate of 50 ml/min, when testing with water. During dynamic testing the pressure dropped to an average of 1.5 bar, this drop in pressure is assigned to the deformation of the tap layer of the packing. The test clearly indicated that the packing material is extruded out of the gap due to movement of the SOCCS casing. The test in combination with wireline fluid proved to be more successful. The fluid compresses the compression packing quick then water. In addition the anti-extrusion rings prevented the deformation of the packing material and eventually extrusion out of the housing, therefore the seal was also capable of holding 200 bar pressure dynamically.

It can be concluded that the quickest way of success is to further develop the compression packing in combination with an oil-based viscous fluid. The experiments have shown it is possible to fabricate an oil-based fluid with Newtonian fluid properties, but still achieve viscosities >1000 cP. Using a fluid with shear thinning properties will make it more difficult to control a constant pressure during in dynamic operations.

# 7

## Recommendations

All concepts failed to perform under the necessary requirements as set at the beginning of the study. The initial concepts did however show both positive and negative effects during testing, a lot of ideas for new concepts or future tests have been thought of in the end. Since there is a clear discrepancy between recommendations for the university and what would be the way forward for Shell, the recommendations are discussed separately.

### 7.1. Recommendations for Future Research

A better understanding of the rheology properties of the fluid is essential to know the limits of the Non-Newtonian Yield Stress Plug concept. A first step would be to incorporate the time-dependent fluid properties as well in the model. Afterwards the eccentricity and geometry of the SOCCS casing can be included. The assumption now is that the stinger will be hovering exactly in the middle of the SOCCS casing, which is assumed to be perfectly round at 101.6 mm. These assumption are represent a advantageous picture compared to reality, in which there is eccentricity and the SOCCS casing is not perfectly round.

To completely validate the model multiple experiments should be performed, in which gap size, length, pressure & flow rate are altered. After validation it is possible to design a configuration in which the concept works. Apart from that it is interesting to combine this concept with a brush seal, which can be modelled as a semipermeable layer. In reality the brush seal would decrease the gap and act as a labyrinth through which the fluid should move, evidently requiring more pressure.

However the CFD model showed it was not possible to model the instability at high pressures. In section 5 it was concluded that this instability was caused by the compressing of the molecular structure of laponite, this also needs to be examined further before relying on a CFD model. Questions that can be answered for further research are:

- Does the mixture of water and laponite has a volume reduction if pressurized in a cylinder?
- At which pressures does the molecular structure break due to compression and how does this relate to different suspensions containing various concentrations of laponite particles?
- Is it possible to measure this phenomenon with help of dielectric spectroscopy?
- Is there a relation between the compression of the molecular structure of laponite discs and the repulsion of single laponite molecules with each other?

It would also be possible to measure this in the set-up, if along the length of the annular gap different pressure sensors would be mounted. This would then tell how the pressure is formed in the fluid, if it will be a constant pressure drop over the entire length or if the pressure is formed up to a certain point a clogging up of fluid.

Since the required application in the SOCCS technology requires very high pressure, this concepts needs to be stretched to its limits in order to work. But the principle of obtaining a very viscous fluid almost instantly through a double precipitation reaction could be interesting for other applications as well.

The success of the swellable rubber, either in oil or water, greatly depends on the final swelling pressure as function of the swelling ratio. This not only determines the probability with which the seal would leak but the friction force is also depended on this aspect. If further research is done for this concept this could be tested through measuring a blocking force from constrained swelling. An extensive knowledge on elastomers and its behaviours is also necessary to obtain a solution in which the properties are favourable. The EPDM swelled rubbers in base oil already show a big decrease in material hardness, which is expected to be very problematic in full scale test. Not only will the rubber seal deform under the high pressure and form a leak path for the fluid, but also a change of extrusion is very likely along with unfavourable wear properties.

A more detailed look into the rheology properties of the engineered base oil will pay off for every concept. The Newtonian like behaviour makes is a lot easier for the understanding of flow through an annulus in these conditions. It is also very interesting to use these types of fluid in combination with other concepts.

Both the compression packing as the chevron seal were an industry ready concept, so further development of these concept would not involve any extensive research. If further tested the main focus should be to look at wear properties of the material and designing of the housing for the concepts.

## 7.2. The Way Forward for Shell

It will be wise for Shell to take a better look at the tests done with base oil, the time spend would be an investment for any other concept. In potential this fluid could also be used as a standalone concepts, only using the stinger design with a pipe OD of 100 mm, since it follows the Hagen-Poiseuille equation.

Further developing an oil-based fluid is preferable to further research into a water-based fluid, such as a mixture containing laponite, since in practice the shear thinning effects will create problematic operational requirements. During the full-scale experiments already some drawbacks of this solution came to light, such as:

- Settling of laponite particles in mixture clogs the flow tubes and makes it difficult to use in certain pumps.
- Once the fluid is flowing the viscosity will only decrease more, due to the shear thinning effect. The pumps will therefor need to be able to have a large flow rate capacity to counter this effect.
- Due to the time-dependent property of the laponite mixture, the buildup pressure can suddenly change. Maintaining the pressure at 200 bar in the pressure chamber could prove to be very difficult.

It is recommended to further develop a solution with compression packing, the obtained results were well within the requirement set out from the start of the research. The results were obtained during only one single try and it is necessary to repeat this test and to look at the wear related issues if the concept is subjected to a long distance test. Because there is still more room for improvement of this solution, since more experiments can be performed with the oil-based fluids that were made for oil swellable rubbers. With the possibility to further optimize this solution it is clear that this is the most promising concept and can be easily made into a final design.

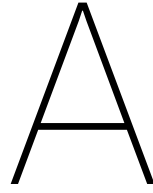
There are opportunities to further develop a concept with a chevron seal, because works on the principle of a self-activating seal in case of higher pressure. The drawbacks of this concept still are related to wear, since it as a full contact seal. A study for which material would suit the application best is required to determine a final concept, which can easily be done in the required test set-up. Another option to enhance this concept is to put multiple chevron seals in series, if one fails due to wear another seal can takeover to enable redundancy.

A hybrid solution using chevron and a swellable rubber is also proposed as a viable solution. The concept is based on chevron V-rings, with the openings of the V-rings opposite to each other, which encircle an EPDM O-ring. The EPDM O-ring swells in the base oil and thus opens the V-rings of the chevron set, if leakage occurs the seal will heal overtime. While the V-rings will keep the O-ring in place and prevent extrusion.

# Bibliography

- [1] P. Bahadur and N.V. Sastry. *Principles of Polymer Science*. Alpha Science International, 2005. ISBN 9781842652466. URL <https://books.google.com/books?id=Z7i1QwKzYiEC>.
- [2] Ron Baker. *Primer of oil well drilling*. 1979.
- [3] H.A. Barnes, J.F. Hutton, and K. Walters. *An Introduction to Rheology*. Annals of Discrete Mathematics. Elsevier, 1989. ISBN 9780444871404. URL <https://books.google.com/books?id=B1e0uxFg4oYC>.
- [4] F.L. Buchholz and A.T. Graham. *Modern superabsorbent polymer technology*. Wiley-VCH, 1998. ISBN 9780471194118. URL <https://books.google.com/books?id=3L9TAAAAMAAJ>.
- [5] H Hugo Buchter. *Industrial sealing technology*. Wiley, 1979.
- [6] John Burke. Part 2. hildebrand solubility parameter. *Solubility Parameters: Theory and application*, 1984.
- [7] S. Choi and L.J. Justice. Water swellable rubber composition having stable swelling property at high temperatures, October 17 2013. URL <http://www.google.com/patents/US20130269787>. US Patent App. 13/447,611.
- [8] N.C.B.P.D.H.O.S.O. Dril. *Deep Water: The Gulf Oil Disaster and the Future of Offshore Drilling: Report to the President, January 2011: The Gulf Oil Disaster and the Future of Offshore Drilling*. US Independent Agencies and Commissions, 2011. ISBN 9780160873720. URL <https://books.google.com/books?id=zDhMtUKWAPsC>.
- [9] Robert K Flitney. *Seals and sealing handbook*. Elsevier, 2011.
- [10] George Neville Greaves, AL Greer, RS Lakes, and T Rouxel. Poisson's ratio and modern materials. *Nature materials*, 10(11):823–837, 2011.
- [11] G Loglio, U Tesei, R Miller, and R Cini. Dilational viscoelasticity of fluid interfaces: the diffusion model for transient processes. *Colloids and surfaces*, 61:219–226, 1991.
- [12] R.L. Panton. *Incompressible Flow*. Developmental clinical psychology and psychiatry. Wiley, 1996. ISBN 9780471593584. URL <https://books.google.co.uk/books?id=bm225PBtke0C>.
- [13] E Pruyt. Spm4121: Foundations for engineering design and decisionmaking. *Delft University of Technology*, 2009.
- [14] Antonio Russo and Walter Navarrini. Glass transition temperature, January 1 2002. US Patent 6,335,408.
- [15] W.R. Schowalter. *Mechanics of Non-Newtonian Fluid*. Elsevier Science & Technology, 1978. ISBN 9780080217789. URL <https://books.google.co.uk/books?id=KwNRAAAAMAAJ>.
- [16] Carlos A Smith and Armando B Corripio. *Principles and practice of automatic process control*, volume 2. Wiley New York, 1985.
- [17] G. Verkerk. *Binas: informatieboek vwo-havo voor het onderwijs in de natuurwetenschappen*. Wolters-Noordhoff, 1998. ISBN 9789001893514. URL <https://books.google.nl/books?id=NEt-YgEACAAJ>.
- [18] J.O. Wilkes. *Fluid Mechanics for Chemical Engineers with Microfluidics and CFD*. Prentice-Hall international series in the physical and chemical engineering sciences. Prentice Hall Professional Technical Reference, 2006. ISBN 9780131482128. URL <https://books.google.co.uk/books?id=IgfVvAQAQBAJ>.





## Concepts Overview

This appendix will give an short overview of all the concepts that were taken into consideration for the concept derivation in section 3.2. The seals are divided in a contact- and a clearance seal section.

### A.1. Contact Seals

As mentioned in section 3.1 contact seals have the seal bear against its counterface under positive pressure. Figure A.1 shows three different ways of how a seal can exert the pressure on its counterface. The three possibilities shown in figure A.1 are described below:

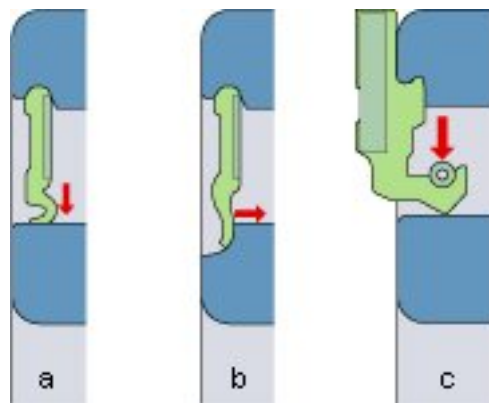


Figure A.1: Options for a seal to exert pressure on its counterface

- The resilience of the seal, resulting from the elastic properties of the seal material (a).
- The designed interference between the seal and its counterface (b).
- A tangential force exerted by a garter spring incorporated in the seal (c).

#### A.1.1. Elastomer Seals

The most common used contact seals are elastomers, or amorphous polymers that exist above their glass transition temperature  $T_g$  [14]. Therefore rubbers or elastomers are relatively soft and deformable at ambient temperature. The polymer seals are designed in a wide variety of shapes, depending on its function, the most common shape is the O-ring as displayed in figure A.2.

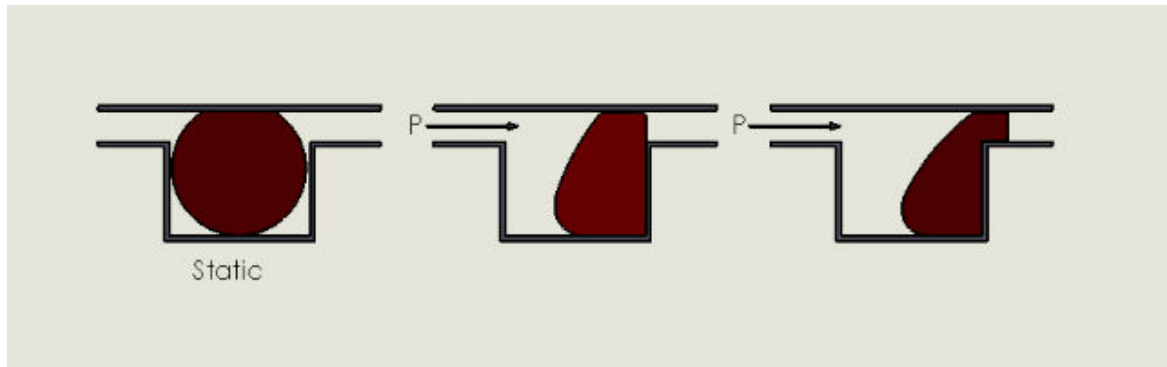


Figure A.2: Cross-sectional shape of O-ring under increasing pressures

Apart from the O-ring there are numerous other types of seals, the ones displayed in figure A.3 are the types that are taken into account for the remainder of this chapter.



Figure A.3: Different types of cross-sectional shapes

### A.1.2. Packing Seals

Compression packing is often known as "packing", the concept is dated back to the beginning of the industrial revolution [9]. Although the packing seal is an old concept, new developments of materials makes it still a popular sealing technique. A packing seal is a series of rings made from a soft material that is compressed in axial direction. Packing seals are manufactured by braiding a fibrous material into a square cross-sectional cord that is cut to length to form the packing, see figure A.4 for different types of braiding.

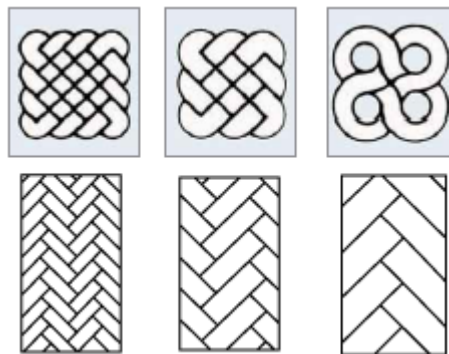


Figure A.4: Different types of braided compression packing

The tighter the material is braided together in the mesh the higher the volume stability of the chord. The fibres can be made from materials, in the majority of cases from: aramid, graphite or polytetrafluoroethylene (PTFE). The decision for a specific material depends on the environment: low/high temperature, aggressive fluids, low/high friction etc.

A typical compression packing seal arrangement will be made up from four or five chord rings. The rings need to be axially compressed to be able to expand on its counterface, see figure A.5.

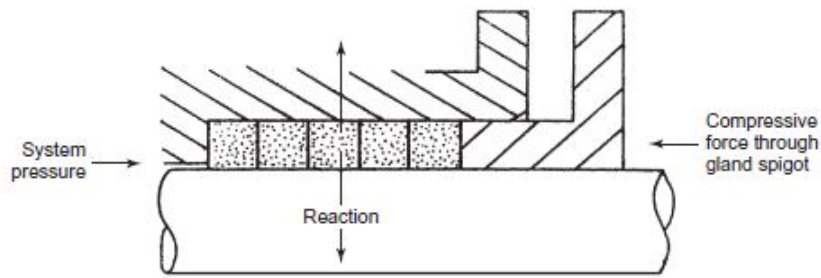


Figure A.5: Cross-sectional view of simple compression packing arrangement

The required number of rings is limited, since the compressive force needs to be translated from the first ring onwards. In most cases 5 rings is used for an adequate distribution of force over the rings, any additional rings installed would not contribute to the sealing force. Figure A.6 shows how the compression force is transferred from beginning to the end.

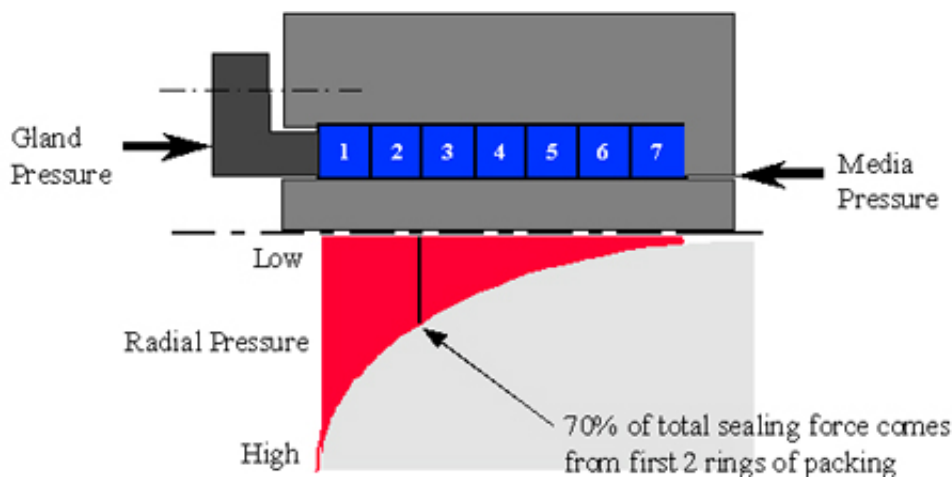


Figure A.6: Radial pressure distributino vs. number of rings in packing seal

### A.1.3. Swellable Rubber

The phenomenon behind swellable rubber is triggered by an osmotic reaction. Osmosis is the tendency of solvent molecules to move through a semi-permeable membrane into a region of higher solute concentration [7]. This reaction occurs from the tendency of a pure solvent to move through a semi-permeable membrane and into a solution containing a solute to which the membrane is impermeable, see figure A.7.

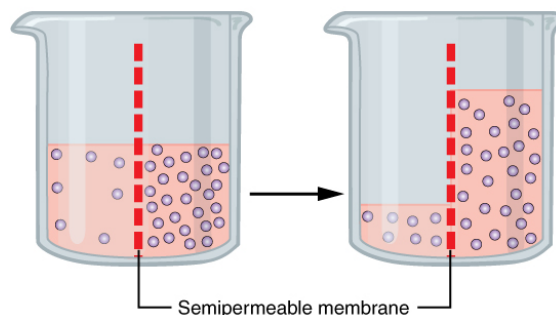


Figure A.7: The process of osmosis over a semi-permeable membrane

Figure A.7 resembles two solutions with a semi-permeable layer in between, in the case of a swellable rubber the rubber acts as the semi-permeable layer. When the rubber was created salts or super-absorbent polymers (SAP's) have been added to its liquid form, when hardened the particles are distributed over the rubber. When the rubbers comes into contact with water the salt/SAP has the tendency to move to the water which contains a lower concentration of salt/SAP. Water molecules travel the opposite direction and nestle in the empty pockets in the rubber, the water particles are larger and force the rubber to expand and thus the rubber grows. The rubbers swells in such a way that it will form itself against the profile of its counterface, thus completely sealing a gap.

The corresponding growth rate and osmotic pressure that can be achieved depends on the type of salt or SAP, temperature and concentration salt/SAP of the surrounding water. This phenomenon is also used in a toy as displayed in figure A.8.



Figure A.8: Example of a plastic toy that swells when in contact with water

The osmotic pressure can be calculated using the Jacobus H. van 't Hoff equation, which Harmon Northrop Morse extended to the following equation:

$$\Pi = i[M]R_{gas}T \quad (A.1)$$

In which  $i$  is a dimensionless correction factor,  $[M]$  is the number of moles of solute in the solution divided by the solution volume or  $mol/ltr$ . The gas constant is represent by  $R_{gas}$  in  $Jmol^{-1}K^{-1}$  and  $T$  the temperature in  $K$ . The molarity can be calculated using:

$$[M] = \frac{solubility}{M} \quad (A.2)$$

Solubility is the amount of particles that can be saturated in a volume of water or in  $gr/100 ml$  at a certain temperature. The molar mass is denoted as  $M$  with unit  $gr/mol$ .

## A.2. Clearance Seals

Section 3.1 also mentioned that there are seals that do not touch its counterface, the remaining gap is filled with a liquid. This means that there is no sliding interface between the two surfaces, resulting in very low friction forces because only fluid friction is present. In general other fluids are used in these sealing configuration, the main aspect is that the fluids have different fluid properties.

Every clearance seal works according to the following principle of a Newtonian fluid that flows between two surfaces. In continuum mechanics a Newtonian fluid is a fluid in which the viscous stresses arising from its flow, at every point, are linearly proportional to the local strain [12]. This assumption is used in fluid mechanics, where by applying Newton's second law ( $F = ma$ ) to fluid motion the motion of viscous fluids is described with the Navier-Stokes equations. The Navier-Stokes equation for incompressible fluids is:

$$\frac{\partial \mathbf{u}}{\partial t} + (\mathbf{u} \cdot \nabla) \mathbf{u} = -\frac{1}{\rho} \nabla p + \nu \nabla^2 \mathbf{u} \quad (A.3)$$

This equation has to be rewritten to represent the situation as displayed in figure A.9, where a fluid flows through an annular gap. Over a certain length a pressure drop is expected, the equation for this pressure drop is given by the Hagen-Poiseuille in equation A.4 [18].

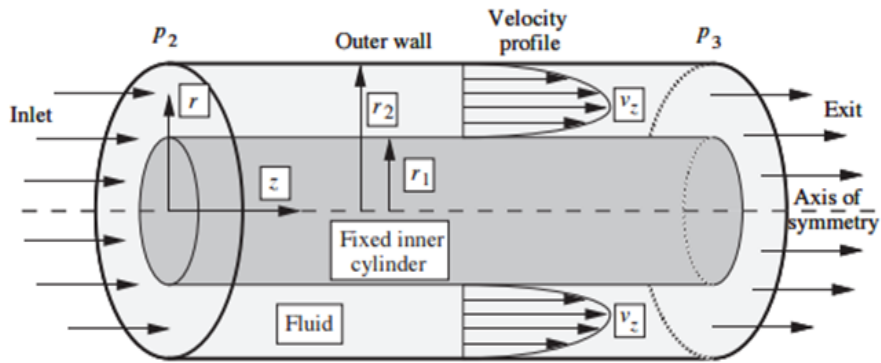


Figure A.9: Geometry of flow through an annular gap

$$Q = \frac{\pi D h^3 \Delta P}{12 \mu L} \tag{A.4}$$

In which  $h = r_2 - r_1$ , or the annular gap between the two pipes and  $\Delta P = p_2 - p_3$ , the pressure drop over the considered length. The derived flow or  $Q$  from equation A.4 can also be described as the leakage rate of the seal. In the remainder of this section the considered clearance seals will be described in more detail.

### A.2.1. Labyrinth Seal

A labyrinth seal functions by providing a distorted path to inhibit leakage. This basically changes the length of the leakpath  $L$  from equation A.4. In order to extend the leakpath the clearance between the labyrinth seal and its counterface needs to be very small, since the fluid needs to be guided through this new leakpath and not just follow the normal path. Labyrinth seals are commonly used in rotary applications. The design of the labyrinth seal plays a role in the effectiveness of the seal, see figure A.10.

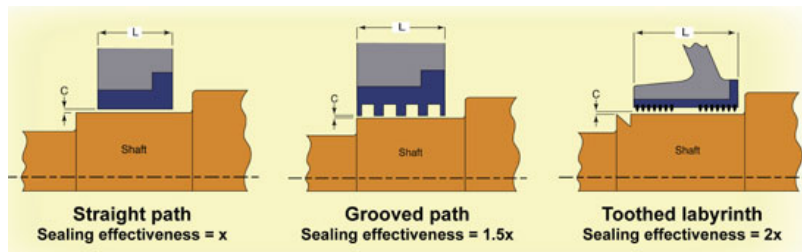


Figure A.10: Different design of labyrinth with corresponding sealing effectiveness

### A.2.2. Brush Seal

A widely used seal for rotary applications is a brush seal, it comprises a series of bristles in a housing which rub on the shaft. The housing is close enough to the shaft to ensure support of the bristles, but sufficiently clear to avoid shaft contact [9]. An example of a brush seal is shown in figure A.11, in this figure the bristles are clearly visible, however there is no housing visible.



Figure A.11: Example of a brush seal

As described the bristles are supported by a housing, consisting of a retaining ring and a backing ring. Figure A.12 shows two different ways of manufacturing a support.

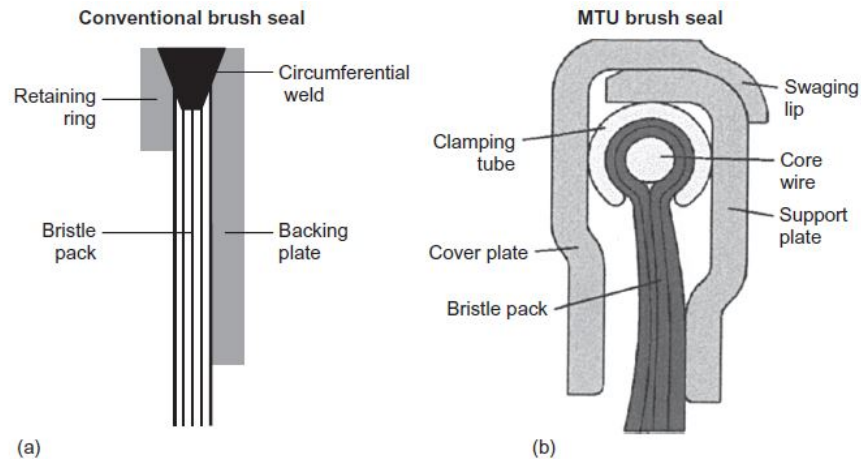


Figure A.12: Basic brush-seal assemblies showing, (a) Conventional brush seal, (b) MTU brush seal

The effectiveness of a brush seal is determined by:

- Material properties of the bristles
- Geometry and positioning of the bristles in the housing and the available gap between the housing and the shaft
- Fluid properties of the sealing fluid

### A.2.3. Non-newtonian Yield Stress Plug

This idea originated from a concept already used in well engineering, specifically during wireline operations. During these operations equipment or measurement devices are lowered into the well for purposes of well intervention, reservoir evaluation or pipe recovery [2]. When lowering down the wireline the well is under pressure and therefore devices are in place to retain the pressure when running the the wireline.

The reason to look at wireline operations is that there are similarities with the seal for the SOCCS technology:

- High pressure, up to 1000 bar from the well
- Low leakage
- Uneven surfaces or the wireline cable, see figure A.13



Figure A.13: Example of uneven surface for wireline braided cable

The clearance seal in the wireline is placed in the stuffing box which houses a flow tube. At the beginning of the flow tube the fluid, in this case a grease, is pumped under a higher pressure than the pressure in the well. The fluid will move both in the well as well as through the flow tube to a point where it exits the flow tube, as shown in figure A.14.

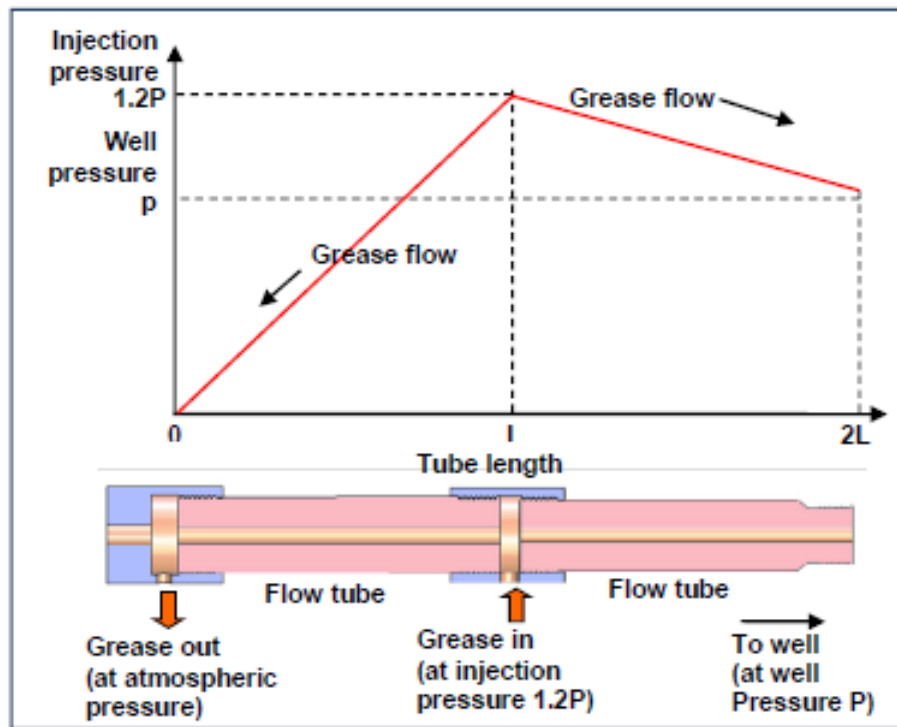


Figure A.14: Pressure gradient in flow tube

The wireline principle works according to the same principle as the Hagen-Poiseuille equation A.4. It showed that it could also be used for high pressure, since most literature does not acknowledge clearance seals to be applicable for high pressure with reciprocating movement [9].

In wireline operations the gap between the braided cable and the flowtube is in the order of 10-100  $\mu\text{m}$ . In section 3.1 it was already clear that due to the out of roundness of the SOCCS casing and the weld the minimum achievable gap would be in the order of 0.5-1.2 mm. Secondly the available length in the SOCCS technology is limited to a maximum of 3 m. The entire set-up of stuffing boxes in wireline operations can easily exceed up to 10 meters.

Therefore it was necessary to look at other parameters of the Hagen-Poiseuille equation that could be altered, which is the viscosity of the fluid  $\mu$ . During wireline operation an oil based grease is used that has a viscosity ranging from 100-1500 cP; water at 20  $^{\circ}\text{C}$  has a viscosity of 1 cP. So to a dramatic increase in viscosity is needed to overcome the gap in the SOCCS technology. A possibility arises when looking at Non-Newtonian fluids instead of regular Newtonian fluids.

The study of the flow of matter, primarily in a liquid state, but also as "soft solids" or solids under conditions in which they respond with plastic flow rather than deforming elastically in response to an applied force [15]. Rheology describes both Newtonian as Non-Newtonian fluids, with Newtonian fluids having only a single coefficient of viscosity for a specific temperature. While Non-Newtonian fluids are characterized by relating stresses with rate of change of strain. Figure A.15 shows general relations between shear stress and shear strain of fluids. Viscosity is calculated by dividing the shear stress with the corresponding shear strain, or:

$$\eta = \frac{\tau}{\dot{\gamma}} \quad (\text{A.5})$$

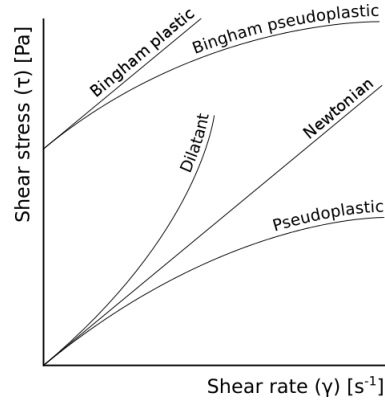


Figure A.15: Classification of fluids with shear stress as a function of shear rate

This represents the resistance to shearing flows, where adjacent layers move parallel to each other with different speeds. This can be defined by the idealized situation in the Couette flow, where a layer of fluid is trapped between two horizontal plates, one fixed and one moving horizontally with a constant velocity  $v$ . Figure A.16 gives the 2D situation of a Couette flow.

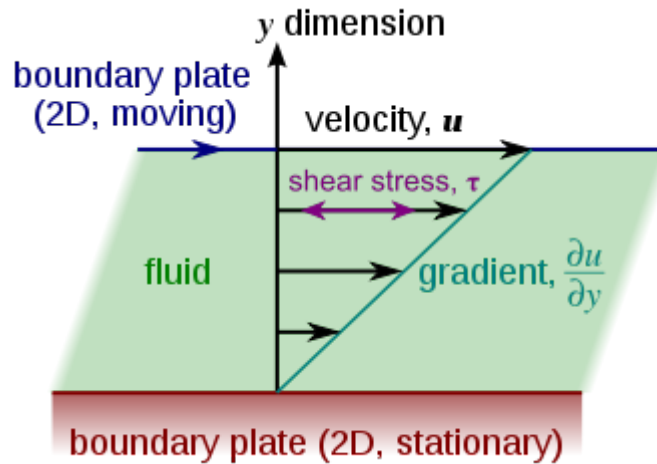


Figure A.16: 2D visualisation of Couette flow

Equation A.5, based on figure A.16, can be rewritten to:

$$\eta = \frac{\tau}{\frac{\partial u}{\partial y}} \quad (\text{A.6})$$

The most interesting Non-Newtonian fluid is the Bingham pseudo-plastic fluids, or fluid which act as a solid but only when reaching a specific stress or yield stress ( $\tau_y$ ). In theory this changes the fluid flow of Hagen-Poiseuille to a plug flow in stationary conditions. The equation for the plug flow can be described by an equilibrium of forces:

1. The force resulting from the pressure:  $F = \sigma A$
2. The opposing friction force resulting from the fluid friction with the surfaces of the inner and outer pipe

The resulting equilibrium of forces is translated to a equation that calculates the required shear stress of the fluid:

$$\tau_{min} = \frac{\Delta P(r_o - r_i)}{2L} \quad (\text{A.7})$$

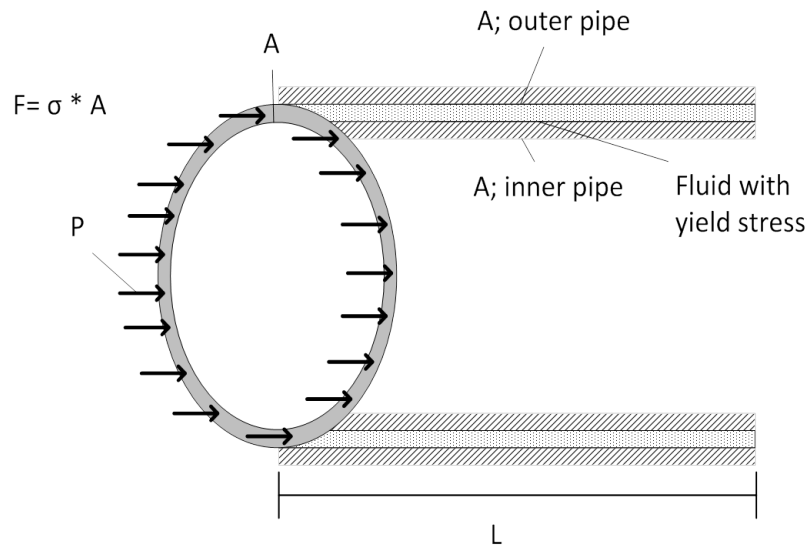


Figure A.17: Equilibrium of forces for a fluid with a yield stress

**A.2.4. Ferro-Fluid Seal**

Magnetic fluid seals, or ferro-fluids seals, are commonly used in rotary seal in vacuum applications or as high-integrity gas sealing [9]. The magnetic fluid seal benefits from low levels of maintenance and very low leakage with hardly any friction or wear. The principle is that the ferro-fluid is suspended in place by use of a permanent magnet, as displayed in figure A.18.

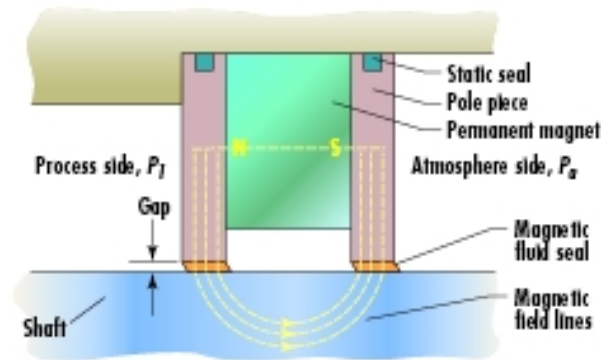


Figure A.18: Principle of a magnetic fluid seal



# B

## Concept Derivation Methodology

This appendix provides the background information and detailed evaluation matrices of the Elimination and Choice Expressing Reality (ELECTRE) method.

### B.1. Criteria Evaluation

The criteria have been determined looking at requirements for the technology and have been verified with Shell engineers. Afterwards the relative importance of the criteria is established by making a pair-wise evaluation of all criteria with each other and to evaluate in ordinal fashion whether criterion  $x$  is *significantly less, less, equally, more* or *significantly more important* than criterion  $y$ , see table B.1. This information is transformed so that every criterion has a certain "weight factor", that can be used in the ELECTRE method.

Table B.1: Performance value function for relative criteria weight

Relative Importance of Criterion x compared with y	Score	Value
(1) Significantly Less Important	1	0.1
(2) Less Important	2	0.3
(3) Equal	3	0.5
(4) More Important	4	0.7
(5) Significantly More Important	5	0.9

The criteria mentioned in table 3.4 are explained in more detail below:

- **Wear:** The ability of the seal to withstand wear resulting from sliding of the seal surface with the SOCCS casing. The seal must be able to perform over the length that is necessary to drill a well, a typical length would be 4-5 km.
- **Coop with surface geometry:** Due to the out of roundness and the sharp edge of the weld in the pipe the seal has to close of the entire annular gap. Therefore the design of the seal has to be flexible enough to overcome this gap.
- **Coop with roughness:** Because there is no real possibility to tread the sliding surface of the SOCCS casing to improve the friction coefficient, the friction coefficient of the material should be low enough to have a good sliding surface.
- **Leakage:** The ability of the seal to close the gap and prevent leakage through the seal. Minimal leakage is accepted if it does not intervene with the welding process.
- **Costs:** The design of the seal should be feasible enough to be able to design and construct during the graduation thesis.
- **Friction:** The friction force of the seal should be within the set requirements. This ensures that the technology in the field can handle these forces, so a seal design can quickly be implemented in the field.

In figure B.1 the criteria have been evaluated using the criteria weight factor from table B.1. The resulting Normalized Weight Factor is the number that is used in order to calculate the overall score of a concept.

Criteria Evaluation Matrix							
	Costs	Friction	Leakage	Wear	Geometry	Roughness	Total
Costs	4	5	4	5	4		
Friction	2	5	3	4	3		
Leakage	1	1	2	3	1		
Wear	2	3	4	3	2		
Coop with surface geometry	1	2	3	3	2		
Coop with roughness	2	3	5	4	4		
Total Points	1.1	1.4	3	2	2.4	1.2	11.1
Normalized Weight Factor	0.099	0.126	0.270	0.180	0.216	0.108	1.000
Normalized Weight Factor (%)	9.9%	12.6%	27.0%	18.0%	21.6%	10.8%	100%

Figure B.1: Criteria evaluation matrix

## B.2. Concept Evaluation

The concepts from section 3.1 have to be evaluated based on their score for every criteria. The concepts can achieve a score on a scale of 0 to 100, with 0 being the worst and 100 the highest score.

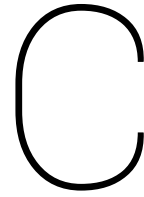
Concept Evaluation Matrix								
#		Costs	Friction	Leakage	Wear	Geometry	Roughness	Total
1	O-ring	85	40	50	15	30	30	250
2	U-ring	75	45	60	20	40	40	280
3	X-ring	80	40	50	15	50	35	270
4	Lip seal	80	45	50	15	40	40	270
5	Chevron/V-packing	70	70	60	25	70	45	340
6	Compression Packing	90	70	90	35	30	50	365
7	Swellable Rubber	80	50	90	60	40	50	370
8	Labyrinth seal	50	80	5	60	60	80	335
9	Brush Seal	30	90	10	65	75	85	355
10	Non-Newtonian Yield Stress Plug	40	95	10	95	95	90	425
11	Ferro Fluid seal	5	80	20	80	20	70	275

Figure B.2: Concept evaluation matrix

The score per concept are displayed in figure B.2. The score for every independent criteria is then multiplied with the Normalized Weight Factor from figure B.1. The result is an absolute score for every concept, as displayed in figure B.3.

Absolute scorecard of concepts								
#		Costs	Friction	Leakage	Wear	Geometry	Roughness	Total
1	O-ring	8.42	5.05	13.51	2.70	6.49	3.24	39.41
2	U-ring	7.43	5.68	16.22	3.60	8.65	4.32	45.90
3	X-ring	7.93	5.05	13.51	2.70	10.81	3.78	43.78
4	Lip seal	7.93	5.68	13.51	2.70	8.65	4.32	42.79
5	Chevron/V-packing	6.94	8.83	16.22	4.50	15.14	4.86	56.49
6	Compression Packing	8.92	8.83	24.32	6.31	6.49	5.41	60.27
7	Swellable Rubber	7.93	6.31	24.32	10.81	8.65	5.41	63.42
8	Labyrinth seal	4.95	10.09	1.35	10.81	12.97	8.65	48.83
9	Brush Seal	2.97	11.35	2.70	11.71	16.22	9.19	54.14
10	Non-Newtonian Yield Stress Plug	3.96	11.98	2.70	17.12	20.54	9.73	66.04
11	Ferro Fluid seal	0.50	10.09	5.41	14.41	4.32	7.57	42.30

Figure B.3: Absolute scorecard of concepts



# Experiment Set-Up

In order to test different sealing concepts it is required to design an experiment. The design of the experiment set-up comprises the following stages:

- |                                     |             |
|-------------------------------------|-------------|
| 1. Structural Design                | Section C.1 |
| 2. Measuring environment            | Section C.2 |
| 3. Experimental Set-Up Calculations | Section C.3 |

## C.1. Structural design

A pragmatic approach is taken to design the set-up. Since the experiment is done in a real scale environment, the governing geometry is the SOCCS casing as mentioned in 3.1.2.

In reality the SOCCS casing is made by the pipe mill from a steel plate on a spool. While the spool unwinds the casing is formed and pushed in the well hole. In the experimental set-up only pre-made SOCCS casings will be used, so a continuous movement of casing in 1 direction is not possible. Therefore it is decided to work with a limited pre-made SOCCS casing that is subjected to a reciprocating movement. In order to determine the total length of the set-up it is necessary to look at some different aspects of the set-up, these aspects are discussed in the sections below.

### C.1.1. Pressure chamber

First it is important to look at the length of the pressure chamber to determine the total length of the set-up. As mentioned in section 3.1 a maximum kick can occur with a pressure of 200 bar. The fluid in the pressure chamber needs to be pressurized to at least 200 bar, to counter the potential kick during drilling. Because the pressure and the ID of the SOCCS casing are known a rule of thumb can be used to estimate the length of the pressure chamber.

As a rule of thumb the ratio between the length and the diameter of a pressure chamber in a pipe is:

$$\frac{length}{diameter} \approx 6 \tag{C.1}$$

The pressure chamber for the set-up will be:  $101,6 * 6 \approx 600mm$ .

### C.1.2. Dynamic actuator

As mentioned in the section above the decision is made to go for a reciprocating movement. The question still remains if the SOCCS casing or the flow-return pipe moves in the test set-up, since it has a large effect on the total size of the set-up.

Moving of the inner flow-return pipe will greatly reduce the overall size of the set-up. Since the length necessary to achieve a certain stroke is less then when moving the outer SOCCS casing, see figure C.1.

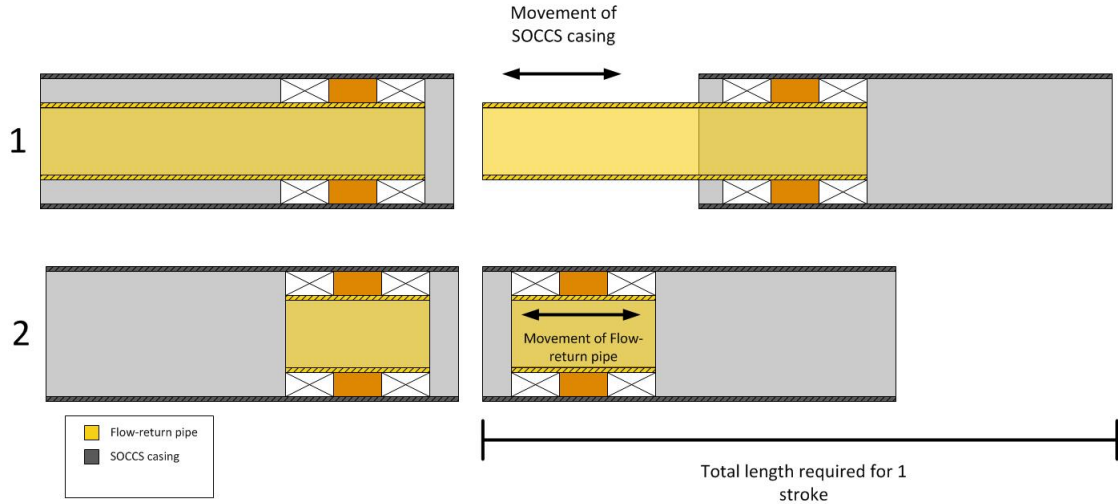


Figure C.1: Movement of parts compared to total size of set-up

1. Movement of outer SOCCS casing
2. Moving of inner flow-return pipe

Before an option for movement can be chosen a decision still needs to be made how the movement will take place, so multiple options for a dynamic actuator were taken into consideration:

- Piston cylinder
- Steel wire
- Chain
- Rack & pinion

Through a discussion with people from the experimental support department of Shell, valuable insight and understanding of every option was achieved. Because it was important to know how practical an option would be in reality. Apart from practicality factors as costs, delivery time and availability were also taken into account. In the end the decision was made to go for a reciprocating movement with the help of a chain.

Still the type of movement needed to be decided, either the movement of the SOCCS casing or the flow-return pipe. Again after an discussion with people from the experimental support it was chosen to go for a set-up in which the SOCCS casing was moving. Firstly because the dimensions of the chain are too large to fit in the SOCCS casing. A second advantage was that the tubes through which the fluid is transported could remain stationary during experiments.

In figure C.2 an overview of the designed experimental set-up is given. In which the flow-return pipe is stationary and as an orange colour. For the remainder of the report the flow-return pipe will be named the stinger, more information in section C.1.3. The SOCCS casing is supported on a plate, which is connected with the chain that provides the reciprocating movement.

### C.1.3. Stinger design

As mentioned in section C.1.2 the stinger represents the flow-return pipe. The main purpose of the stinger in the experimental set-up is to:

- Provide space to install the sealing configurations and the pressure chamber
- Centralize in the SOCCS casing
- Be able to cope with the friction forces on seals
- Guide and protect the flowtubes that supply the fluid to the pressure chamber

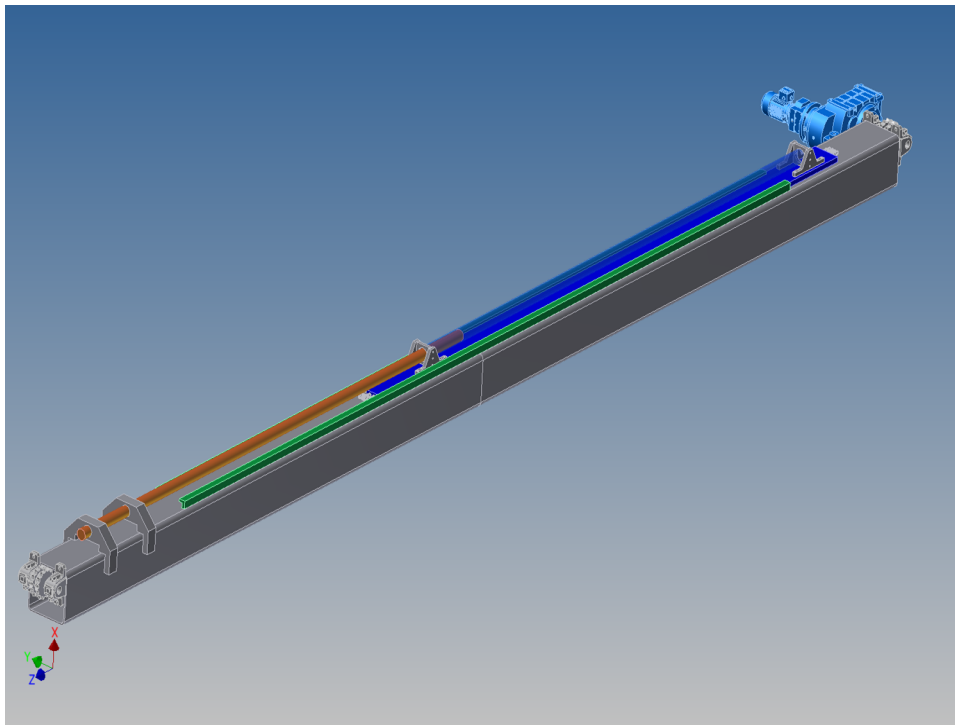


Figure C.2: Overview of designed experimental set-up

In order to have a practical set-up it was important that it would be easy to switch between different sealing configurations. Because the configurations had to be mounted on the stinger, the stinger pipe had to consist of multiple interchangeable components, see figure C.3.

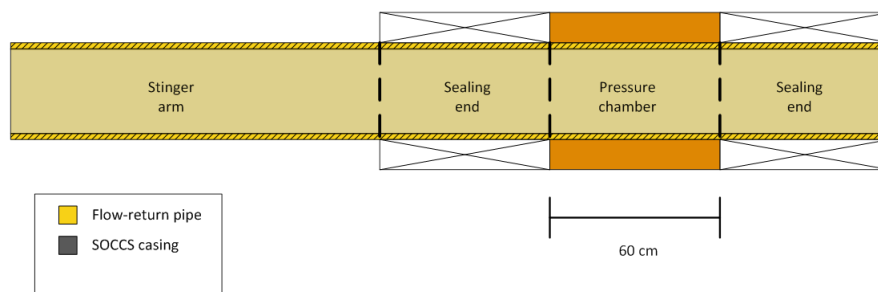


Figure C.3: Overview of stinger components

The purpose was to design the entire stinger with connections that could easily be disconnected but still be able to withstand the axial force due to the friction of the seals. The decision was made to go for threaded connections between the 4 parts of the stinger.

The flowtubes would run through the stinger end and the left sealing end, which are hollow pipes. And then they would be connected to the pressure chamber part. The design of the remainder of the sealing ends will be discussed in chapter 4, since it depends on the sealing configuration how the parts will look.

## C.2. Measurement environment

Apart from all the structural design measurement also need to take place during the experiments. In section 3.1 of this chapter the operational conditions of a test are given in table 3.1. Because the set-up is in scale with reality the geometry & surface roughness conditions is met. The motor which drives the chain is able to to from  $0,4 \text{ m/s}$  to  $1,5 \text{ m/s}$ , so the condition of the speed is also met. That leaves the 3 main parameters that should be measured during the experiments:

1. Friction
2. Leakage
3. Wear

As mentioned in section 3.1 wear is assumed to be a function of friction and leakage over time, so no extra measurement devices are implemented. The other parameters are discussed in the following sections.

### C.2.1. Friction

A friction force originates as a resistive force between relative motion of multiple surfaces. The term surface can relate to either solid, fluid or gas, a combinations between different types of surfaces is also possible. During the experiments friction will occur between the sealing configuration and the SOCCS casing. The friction force is transferred to an axial force on the stinger, so at the position where the stinger is mounted on the frame a horizontal reaction force occurs. Figure C.4 gives illustrated example.

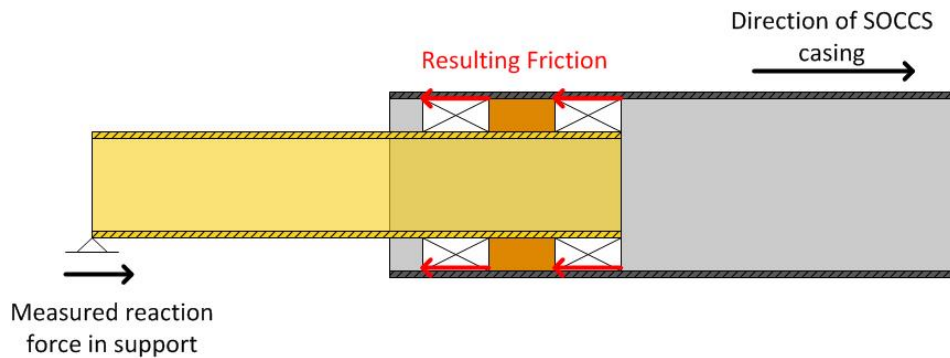


Figure C.4: Transferred friction force to reaction force in support

The friction force will be measured by two S-beam load cells, which can both measure tension and compression. The cells will be positions on the mounted stinger end on the set-up, as displayed in figure C.5. The capacity of a single load cell is up to 50 kN, since the maximum allowable friction force for the set-up has been designed for 5 tons.

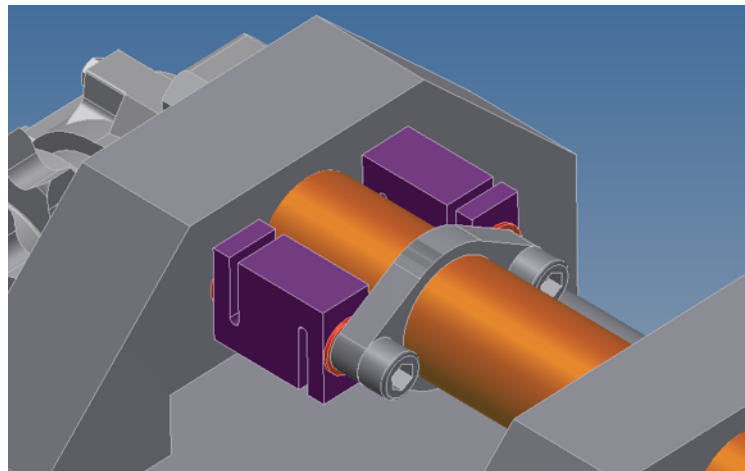


Figure C.5: Position of S-beam on set-up

The specifications of the load cell is given in table C.1.

### C.2.2. Leakage

The primary goal of the seal is to block the leak path between the flow-return pipe and the SOCCS casing. Therefore leakage is an important parameter to measure during the experiments, since it determines if a

Table C.1: Specification S-beam load cells

Specifications	Value
Rated capacity [tons]	5
Combined Error [% of R.O.]	0.035
Non-Repeatability [% of R.O.]	0.015
Minimum Division Size [ $v$ min., % of R.O.]	0.030
Temperature Coefficient	
Output [ppm/ $^{\circ}$ C, of load]	16
Zero [ppm/ $^{\circ}$ C, of R.O.]	42
Creep Return [% of load, 30 Min.]	0.050
Rated Output [mv/v]	$3 \pm 0.25\%$
Zero Balance [% of R.O.]	$\pm 2$
Excitation [Volt]	10 recommended, 15 Max.
Input Impedance [ $\Omega$ ]	$385 \pm 10$
Output Impedance [ $\Omega$ ]	$350 \pm 1\%$
Operating Temperature Range [ $^{\circ}$ C]	-40 to +60
Environmental Protection [DIN]	IP65
Safe Overload [% of R.O.]	150
Deflection [mm, @ Rated Capacity]	0.40

concepts functions or not. Leakage will be measured in the amount of volume that is lost during a specific time, for example in  $ltr/hr$ . The easiest way to measure the amount of volume lost is to measure the amount of volume that goes into the pressure chamber over time. The only way the fluid can go out of the system is to go past the sealing configuration.

This is achieved by designing a closed system which supplies the fluid to the pressure chamber and is also possible to measure volume transported to the pressure chamber. A certain pressure needs to be maintained in the pressure chamber during the experiments. Both conditions are achieved by the use of two Quizix pumps, which can either be instructed to pump to achieve a certain pressure or pump a certain flow rate. In figure C.6 an overview is given of the 2 pumps that supply the flow rate to the pressure chamber. If the pressure chamber is maintained on a certain pressure then the flow rate needed to maintain this pressure is the leakage past the seals.

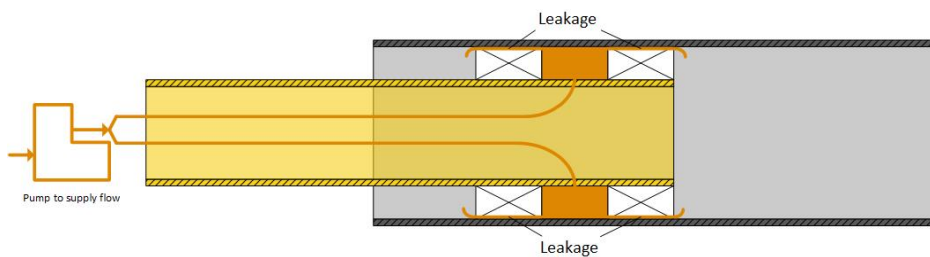


Figure C.6: Overview of pump usage in set-up

The decision was made to use two Quizix pumps, which are readily available within Shell. Each pump consists of 2 pistons which can independently extrude and retract. Therefore these pumps can easily maintain a certain pressure by continuously pumping a certain flow rate.



Figure C.7: Quizix QX 6000

The specifications for the Quizix QX 6000 pumps are given in table C.2.

Table C.2: Specification Quizix QX 6000 pump

Specifications	Value
Max Pressure [bar]	413
Max Flow Rate [ml/min]	50
Cylinder Stroke Volume [ml]	12.3
Minimum Flow Rate [ml/min]	0.001
Accuracy [% of flowrate]	0.1

Figure C.6 clearly shows that there the pumps are located at a certain distance of the pressure chamber. So the pumps need to regulate the pressure in the pressure chamber, while compensating for the pressure losses in the flow tubes. A wide range of different fluids will be used in the set-up, so the pressure losses due to friction in the flow tubes is hard to predict. Therefore it is easier let the pump regulate the pressure in the pressure chamber directly. This is done by installing a pressure sensor in the pressure chamber, the position of the sensors can be viewed in figure C.8.

The fluid enters the pressure chamber just to the right of the pressure sensor on the right of the figure. This sensor gives the highest pressure inside the pressure chamber and sends this as an input back to the Quizix pump. The second pressure sensor is merrily added to measure the pressure at the end of the pressure chamber, just before the fluid enters the sealing configuration. The difference between the two sensors gives an indication of the pressure loss within the pressure chamber during experiments, since it is a goal to maintain a constant pressure over the entire chamber.

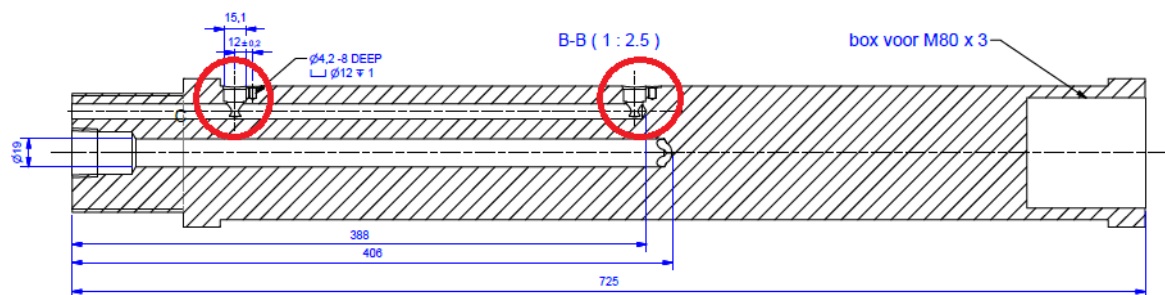


Figure C.8: Position of pressure sensors in pressure chamber

The sensors needed to be able to coop with extremely viscous fluids, so the decision was made to go for piezoresistive OEM Pressure Transducer from Keller. A picture of a sensor can be viewed in figure C.9.



Figure C.9: Example of piezoresistive pressure sensor from Keller

The specifications for the Keller pressure sensor are given in table C.3.

Table C.3: Specification Keller piezoresistive pressure sensor

Specifications	Value
Min Pressure [bar]	2
Max Pressure [bar]	200
Accuracy [% of FS]	typ. < 0.25, max. < 0.5

### C.2.3. Additional measurements

Apart from the already mentioned measurement devices in place, there are also a number of parameters that are helpful is measured. The parameters are mentioned below and briefly explained in this section.

- Length of stroke
- Temperature
- Deformation of of SOCCS casing

#### Length of stroke

The distance over which the SOCCS casing moves gives the relevant stroke. Combined with the time and speed of the moving SOCCS casing accelerations can be calculated. This could be of interest if stick-slip movement occurs during the experiments.

#### Temperature

As a results of friction the kinetic energy of the sliding surfaces gets converted into thermal energy. The thermal energy is then dissipated to the surrounding environment, which could potentially influence the surrounding sealing configuration. A conservative calculation has been done to get an estimate of the increase in temperature, see section C.3. The calculations shows that the temperature does not increase drastically and no precautions need to be taken into account. No temperature measurements are performed from the start of the experiments.

#### Deformation of SOCCS casing

Due to the internal pressure on the SOCCS casing, elastic deformation can occur due to increase in strain. Strain is a measure of deformation representing the displacement between particles in the body relative to a reference length. This phenomena works counterproductive to the sealing configurations. The seals is designed to close or minimize the gap between the two pipes, while the elastic deformation of the outer pipe only increases the gap size. The corresponding calculation is done in section C.3.

### C.3. Experimental Set-Up Calculations

This chapter will discuss calculations that have been performed with regard to the experimental set-up.

#### C.3.1. Buckling force in stinger

As mentioned in figure C.4 as a results of the sliding of the SOCCS casing over the sealing configuration friction can occur. The friction force results in an axial force on the stinger, so the stinger needs to be designed to withstand buckling.

Buckling is considered a sudden sideways failure of a structural member subjected to high compressive stress. At the moment of buckling the compressive stress is less than the ultimate compressive stress that the material is capable of withstanding.

The classic analysis for buckling comes from Euler, given with the formula:

$$F_b = \frac{\pi^2 EI}{L_{eff}^2} \quad (C.2)$$

However in the case of very slender objects buckling can occur below the calculated Euler force, due to shortening of the object. This formula, also known as the Johnson formula, uses a parabolic curve fit to account for failures in the new shortened region.

$$F_b = \sigma_y A \left[ 1 - \left( \frac{\sigma_y}{4\pi^2 E} \right) \left( \frac{L_{eff}}{r} \right)^2 \right] \quad (C.3)$$

Depending on the slenderness of the beam either the Johnson or the Euler formula is used. The stinger has an ID of 70 mm and an OD of 90 mm.

$$R_g = \sqrt{\frac{I}{A}} \approx 29 \quad (C.4)$$

With  $A$  the Area of the cross section of the pipe and  $I$  the Moment of Inertia of the cross section.

$$A = \frac{1}{4} \pi (D_o^2 - D_i^2) \quad (C.5)$$

$$I = \frac{1}{64} \pi (D_o^4 - D_i^4) \quad (C.6)$$

$$S = \frac{L_{eff}}{R_g} \approx 71 \quad (C.7)$$

$$S_{cr} = \sqrt{\frac{2\pi^2 E}{\sigma_y}} \approx 126 \quad (C.8)$$

In equation C.4 the radius of gyration is calculated, which is an input for equation C.7. The calculated slenderness in equation C.7 is less then the critical slenderness of equation C.8, therefore the Johnson formula is used in the remainder of this section.

In order to use the Johnson buckling formula it is necessary to look at the effective buckling length, or  $L_{eff}$ . This depends on the conditions of the end supports of the column. A generalization of these conditions is given in figure C.10.

The experimental set-up relates to the conditions illustrated in figure C.10 (c). The total unsupported length of the stinger is at most 2.9 m, multiplied with the effective length factor the effective length becomes  $2.9 * 0.7 = 2.03$  m. The remaining variables in the Johnson equation C.3 are the Elasticity Modulus  $E$  and the Yield strength  $\sigma_y$ . The stinger is made from regular steel with properties as mentioned in table C.4.

Table C.4: Steel properties of stinger

Specifications	Value
Elasticity Modulus [ $N/mm^2$ ]	200000
Yield Strength [ $N/mm^2$ ]	250

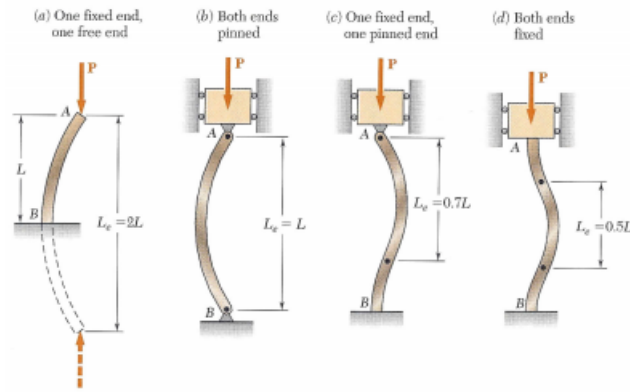


Figure C.10: Effective buckling length related to support conditions

Filling in all the relevant variables in equation C.3 yields a buckling force of  $527 \text{ kN}$ . This limit is high above the maximum pulling force of the chain, which is  $50 \text{ kN}$ . So it can be concluded that the experimental set-up is designed to withstand buckling forces.

### C.3.2. Thermal energy due to friction

In section C.2.3 it was already mentioned that friction could lead to additional heating. In this section a conservative approach is taken to calculate the possible increase in temperature.

First of all it is assumed that all the kinetic energy is transformed to thermal energy which is absorbed by the SOCCS casing. Secondly a very low typical heat transfer coefficient for air is used, of  $10 \text{ W/m}^2\text{K}$ . The third assumption is that the energy is generated over the entire length over which the seal slides, with the ID of the SOCCS casing of  $101.6 \text{ mm}$  and a stroke length of  $4 \text{ m}$ .

$$A = \pi DL \approx 1.28 \text{ m}^2 \quad (\text{C.9})$$

In addition to the already mentioned assumption the situation is taken in which the maximal capable friction force is active, of  $50 \text{ kN}$ . The constant velocity of  $1 \text{ m/min}$  is taken into account for the remainder calculations. The resulting power of a single stroke is calculated through:

$$Q = Fv \approx 833 \text{ W}$$

The generated energy through friction is transferred from the SOCCS casing to the surrounding ambient air, which has a temperature of  $293 \text{ K}$ . The transfer of the heat to the air is done through the convection heat transfer function:

$$Q = \alpha A(T_2 - T_1) \rightarrow T_2 = \frac{Q}{\alpha A} + T_1 \approx 358 \text{ K} \quad (\text{C.10})$$

This results in an increased temperature of the SOCCS casing to a maximum of  $358 \text{ K}$  or  $85 \text{ }^\circ\text{C}$ .

### C.3.3. Deformation of SOCCS casing

During the experiments the SOCCS casing is subjected to an internal pressure and an increasing temperature. This results in circumferential strain in the casing, which leads to a larger radius of the casing. This section covers both effects and serves as an estimate for the increase in radius.

#### Pressure

A cylinder can be described as a pressure vessel which is subjected to an internal pressure. The internal pressure results in several stresses in the cylinder, see figure C.11.

In reality the SOCCS casing has a very long length compared to the diameter, so the assumption is made that only hoop stress is present. The hoop stress is calculated with the following equation.

$$\sigma_H = \frac{PD_m}{2t} \quad (\text{C.11})$$

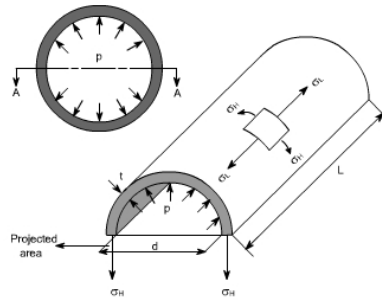


Figure C.11: Axial and hoop stresses in a cylindrical pressure vessel

The corresponding hoop strain is given by Hooke's law as:

$$\epsilon_H = \frac{\sigma_H}{E} = \frac{PD_m}{2tE} \quad (C.12)$$

Since this strain is the change in circumference  $\delta_C$  divided by the original circumference  $C = \pi D_m$  the equation becomes:

$$\delta_C = C\epsilon_H = \pi D_m \frac{PD_m}{2tE} \quad (C.13)$$

The change in circumference and the corresponding change in diameter  $\delta_D$  are related by  $\delta_D = \delta_C/\pi$ , so the expression becomes:

$$\delta_D = \frac{PD_m^2}{2tE} \quad (C.14)$$

In the table C.5 the parameters are given for the equation.

Table C.5: Used parameters in hoop stress calculation

Specifications	Value
Elasticity Modulus [ $N/mm^2$ ]	200000
Pressure [ $N/mm^2$ ]	200
$D_m$ [ $mm$ ]	103.3
Wall Thickness [ $mm$ ]	3.4

Inserting these parameters into C.14 results in an increase of:

$$\delta_D = \frac{PD_m^2}{2tE} \approx 0.16mm \quad (C.15)$$

So the total increase in diameter due to the internal pressure is 0.16 mm.

#### Temperature

In section C.3.2 it was calculated that the maximum temperature the steel could achieve is 358 K, with an ambient temperature of 293 K. It is assumed that linear expansion takes place, with the following equation:

$$D_1 = D_0(\Delta T\alpha + 1) \quad (C.16)$$

An initial diameter is used of 4", or 101.6 mm. The linear expansion coefficient is assumed to be 12  $\mu m/mK$ . So the new diameter of the SOCCS casing becomes:

$$D_1 = D_0(\Delta T\alpha + 1) \approx 101.68mm \quad (C.17)$$

So the contribution of the increased diameter due to temperature is 0.08 mm. Combining this with the effect of pressure, see section C.3.3, gives an effect of 0.24 mm in total.



# Non-Newtonian Yield Stress Plug CFD

In this appendix a more detailed look will be given to the mechanics behind the Non-Newtonian Yield Stress Plug, in order to get a better understanding of the phenomenons that occur during testing. The first section will focus on the CFD simulation, an attempt has been done in the second section to derive an analytical model of the plug flow.

## D.1. CFD Simulations

The programme Comsol Multiphysics is used as a tool to quickly do a CFD simulation. In section D.1.1 an overview of the assumptions and required steps is given. Afterwards in section D.1.2 the results of the CFD simulations are discussed.

### D.1.1. Assumptions

At first the stationary case, without movement of the outer SOCCS casing, is taken into consideration. The following assumptions are made:

1. Only laminar flow in axial direction
2. No eccentricity
3. No out of roundness of SOCCS casing, is assumed to have a constant ID of 101.6 mm
4. Fluid has no time-dependent properties

Due to this assumptions the system can be simplified to the flow of a Non-Newtonian fluid between to parallel plates, with a length of 800 mm and a gap of 0.8 mm. The initial conditions (IC) can be defined as:

1. At Inlet ( $z = 0 \text{ mm}$ ):  $u = \frac{\text{flowrate}}{\text{cross-sectional area}} \text{ m/s}$
2. At Outlet ( $z = 800 \text{ mm}$ ):  $p = 0 \text{ bar}$

The velocity at the inlet is taken from the static experiment as described in section 5.1, in which a mixture containing 20% laponite was used. At the boundary conditions (BC) of the walls the assumptions is no slip, resulting in:

1. At OD of stinger ( $r = 50 \text{ mm}$ ):  $u = 0$
2. At ID of SOCCS casing ( $r = 50.8 \text{ mm}$ ):  $u = 0$

A power-law model is chosen to Non-Newtonian fluid properties based on measurement performed in the rheometer. The data can be fitted with the following equation:

$$\eta = C \gamma^n \tag{D.1}$$

A mixture containing 20% laponite corresponds to a behaviour index of  $n = 0.2256$  and a consistency index of  $C = 2256 \text{ Pa} \cdot \text{s}$ .

The expectation is that the flow will display a plug-like flow, in which the fluid has a high shear rate at the boundary conditions, but almost none at the centre of the gap. Therefore the mesh is chosen so that the distribution close to the boundary conditions is small, to accurately measure the slope of the shear rate and thus the velocity. The mesh is displayed in figure D.1.

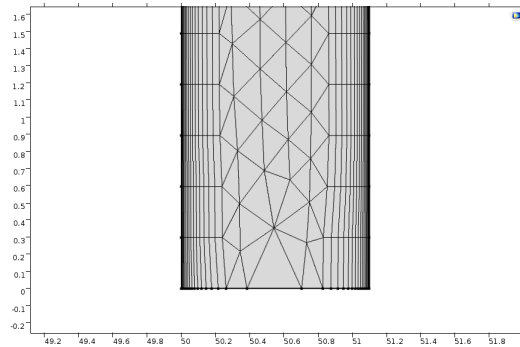


Figure D.1: Chosen mesh for 2D axisymmetric model in Comsol Multiphysics

This mesh proved to be a fairly good representation, since a more detailed would greatly extend the calculation time.

### D.1.2. Results

The expectancy is that the fluid will exhibit a plug-like flow between the two parallel plates. How quickly this plug flow will arise is interesting for further modelling. Figure D.2 displays the velocity of the fluid beginning from the inlet.

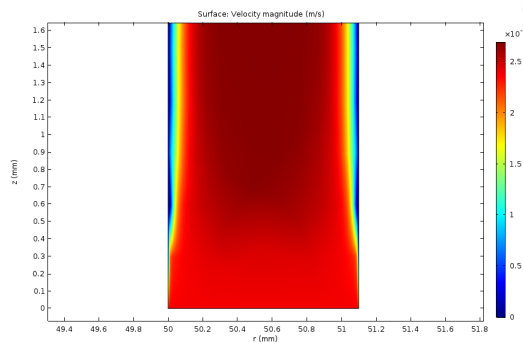


Figure D.2: Velocity magnitude along the surface between the two parallel plates

The figure clearly shows that a fully developed plug flow would occur already after  $z = 1 \text{ mm}$ . The shear rate as function of the radial coordinate is given in figure D.3, at  $z = 1 \text{ mm}$ .

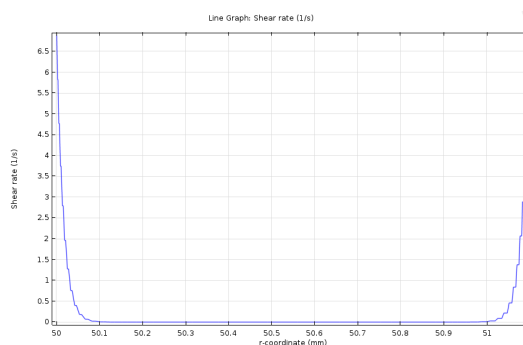


Figure D.3: Shear rate as function of radial coordinate at  $z = 1 \text{ mm}$

Since the shear rate is basically the derivative of the velocity profile between the two plates, the velocity profile is almost constant over the radial length. Only at the BC does the velocity abruptly drop to satisfy the no slip conditions. The velocity profile is shown in figure D.4.

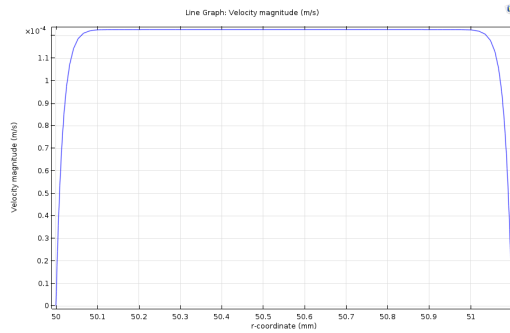


Figure D.4: Velocity as function of radial coordinate at  $z = 1 \text{ mm}$

Profile of the velocity along the entire axial length of the seal is constant it is possible to describe the system in a interval in axial length. This system will be further described in section D.2.

### D.1.3. Dynamic conditions

Also CFD simulations have been performed in which one of the outer wall moved with a speed of 1 m/min. During a dynamic experiments in the set-up two laponite flows in 2 axial direction: either in line with the movement of the casing or opposite to it. The velocity profile when the fluid is flowing in opposite direction as the SOCCS casing is displayed in figure D.5. The obtained pressure gradient in this situation is similar to the pressure gradient in static conditions.

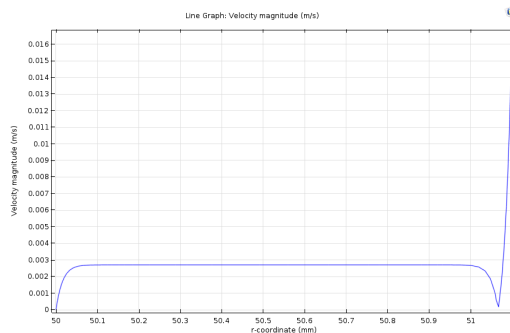


Figure D.5: Velocity as function of radial coordinate at  $z = 1 \text{ mm}$ , during dynamic test with SOCCS casing moving in opposite direction as flow

The velocity profile in the situation that the fluid is moving in the same direction as the SOCCS casing is displayed in figure D.6.

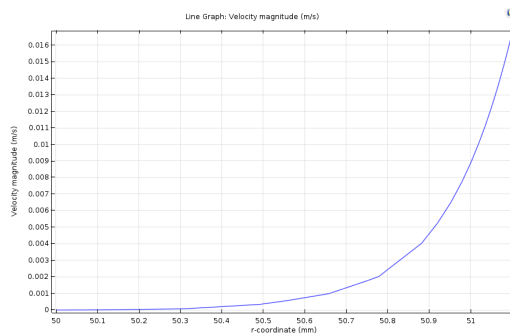


Figure D.6: Velocity as function of radial coordinate at  $z = 1 \text{ mm}$ , during dynamic test with SOCCS casing moving in line with flow

The pressure gradient retrieved from this simulation is different from the one with static conditions. There is no build up of pressure along the gap, it is likely that a certain critical velocity is achieved in this situation. Thereby the fluid is not able to build up pressure anymore.

## D.2. Model

Since in the previous section it is already proven that plug flow will almost instantly occur, it is possible to look at a small section of the fluid as displayed in figure D.7.

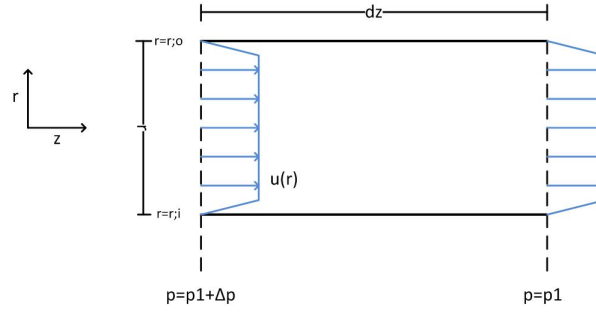


Figure D.7: Plug flow in interval  $dz$

The formula to calculate the pressure drop over the interval  $dz$  is:

$$\frac{\delta p}{\delta z} = \frac{\delta}{\delta r} \left( \eta \frac{\delta u}{\delta r} \right) \quad (D.2)$$

With  $\eta = C \gamma^m$  and  $\gamma = \frac{\delta u}{\delta r}$  equation D.2 becomes:

$$\frac{\delta p}{\delta z} = \frac{\delta}{\delta r} \left( C \left( \frac{\delta u}{\delta r} \right)^{m+1} \right) \quad (D.3)$$

Using  $\frac{\delta p}{\delta z} = \Delta p$  and multiplying both sides with  $r$ :

$$\Delta p r = C \left( \frac{\delta u}{\delta r} \right)^{m+1} \quad (D.4)$$

Introducing a new constant  $C^* = \frac{\Delta p}{C}$ , gives:

$$\left( \frac{\delta u}{\delta r} \right)^{m+1} = C^* r \quad (D.5)$$

$$\frac{\delta u}{\delta r} = \left( C^* r \right)^{\frac{1}{m+1}} \quad (D.6)$$

Integrating equation D.6 over the radial height will result in a function of the velocity of the fluid based on the radial height. In combination with the found values for  $C$  and  $m$  in section D.1.1, this results in:

$$u(r) = \int_{r_i}^{r_o} \left( C^* r \right)^{\frac{1}{m+1}} dr \quad (D.7)$$

No further steps have been taken to derive the analytical model of the velocity profile, this could be done in further research.